lubricants

MDPI

Article

Nano-Enhanced Cactus Oil as an MQL Cutting Fluid: Physicochemical, Rheological, Tribological, and Machinability Insights into Machining H13 Steel

Nada K. ElBadawy [1,*], Mohamed G. A. Nassef [1,2], Ibrahem Maher [2,3], Belal G. Nassef [1,4], Mohamed A. Daha [1], Florian Pape [4,*] and Galal A. Nassef [1]

[1] Production Engineering Department, Faculty of Engineering, Alexandria University, Alexandria 21544, Egypt; mohamed.nassef@ejust.edu.eg (M.G.A.N.); nassef@imkt.uni-hannover.de (B.G.N.); m.daha@alexu.edu.eg (M.A.D.); galalnassef@alexu.edu.eg (G.A.N.)
[2] Industrial and Manufacturing Engineering Department, Egypt-Japan University of Science and Technology, New Borg El Arab City 21934, Egypt; ibrahim.sultan@ejust.edu.eg
[3] Mechanical Engineering Department, Faculty of Engineering, Kafrelsheikh University, Kafrelsheikh 33516, Egypt
[4] Institute of Machine Design and Tribology, Leibniz University of Hanover, 30167 Hannover, Germany
* Correspondence: nada.elbadway@ejust.edu.eg or eng-Nada.kamel1621@alexu.edu.eg (N.K.E.); pape@imkt.uni-hannover.de (F.P.)

Abstract: The widespread use of mineral cutting fluids in metalworking poses challenges due to their poor wettability, toxicity, and non-biodegradability. This study explores cactus oil-based nanofluids as sustainable alternatives for metal cutting applications. Samples of cactus oil are prepared in plain form and with 0.025 wt.%, 0.05 wt.%, and 0.1 wt.% activated carbon nanoparticles (ACNPs) from recycled plastic waste. Plain cactus oil exhibited a 34% improvement in wettability over commercial soluble oil, further enhanced by 60% with 0.05 wt.% ACNPs. Cactus oil displayed consistent Newtonian behavior with a high viscosity index (283), outperforming mineral-based cutting fluid in thermal stability. The addition of ACNPs enhanced the dynamic viscosity by 108–130% across the temperature range of 40–100 °C. The presence of nano-additives reduced the friction coefficient in the boundary lubrication zone by a maximum reduction of 32% for CO2 compared to plain cactus oil. The physical and rheological results translated directly to the observed improvements in surface finish and tool wear during machining operations on H13 steel. Cactus oil with 0.05 wt.% ACNP outperformed conventional fluids, reducing surface roughness by 35% and flank wear by 57% compared to dry. This work establishes cactus oil-based nanofluids as a sustainable alternative, combining recycled waste-derived additives and non-edible feedstock for greener manufacturing.

Keywords: cactus oil; minimum-quantity lubrication; dynamic viscosity; rheological properties; activated carbon nanoparticles

check for updates

Received: 28 May 2025
Revised: 12 June 2025
Accepted: 13 June 2025
Published: 15 June 2025

Citation: ElBadawy, N.K.; Nassef, M.G.A.; Maher, I.; Nassef, B.G.; Daha, M.A.; Pape, F.; Nassef, G.A. Nano-Enhanced Cactus Oil as an MQL Cutting Fluid: Physicochemical, Rheological, Tribological, and Machinability Insights into Machining H13 Steel. *Lubricants* **2025**, *13*, 267. https://doi.org/10.3390/lubricants13060267

Copyright: © 2025 by the authors. Licensee MDPI, Basel, Switzerland. This article is an open access article distributed under the terms and conditions of the Creative Commons Attribution (CC BY) license (https://creativecommons.org/licenses/by/4.0/).

1. Introduction

Sustainable manufacturing has recently been adopted in research since traditional manufacturing systems consume significant levels of energy with low efficiency and depend mainly on non-biodegradable resources [1]. Driven by the rapid increase in economic and business activities, researchers strive hard to convert manufacturing processes to be more sustainable and greener. The concept of sustainable manufacturing comes to the surface as a philosophy with the objective of minimizing the waste and pollution of

manufacturing through sustainable product and process design [2]. The implementation of green manufacturing starts from the selection of raw materials until the final product is finished using clean energy sources, improving manufacturing technology, and using lower-impact materials [3].

Metal cutting fluids are used as lubricants and coolants during manufacturing operations to reduce the heat generated in the workpiece–tool–chip zone. Approximately one-third of the generated heat is caused by external friction of metal-to-metal contact between the workpiece and cutting tool, while two-thirds originate from the internal friction or the resistance of metal structures to the deformation in the shear zone [4,5]. A secondary function of metal cutting fluids is to evacuate chips from the cutting zone and mitigate corrosion mechanisms [6]. Also, physicochemical adsorption and reaction between molecules in the lubricants with the rubbing surfaces take place and reduce the friction of the cutting process [7,8].

Proper lubrication is essential to reduce both external and internal friction in order to reduce process power consumption, extend the cutting tool's life, and enhance the workpiece's surface integrity [9]. The selection of a suitable cutting fluid is crucial, as machining processes widely utilize diverse types, primarily classified into oil-based and water-based cutting fluids, as classified by DIN 51385. Base oils are categorized into mineral oil, synthetic oil, and vegetable oil, with mineral oil-based cutting fluids being the most widely used, accounting for approximately 85% of the total production volume in the market [10]. Mineral oil-based cutting fluids are straight oils with around 15% additives including sulfur and phosphorus compounds as extreme pressure (EP) additives, while other ingredients such as chlorinated paraffins help improve lubricity and friction behavior. Water-based fluids, on the other hand, are mineral oils emulsified in water, which acts as an agent to suspend the additives for efficient performance. While the thermal conductivity of water-based fluids is higher compared to the cutting oils, the friction of the oils is generally lower [11].

Due to the presence of these toxic and hostile ingredients, safety hazards in terms of health and environment impose critical challenges to the application of mineral oil-based cutting fluids in sustainable manufacturing processes [12]. It is estimated that skin contact with fluids contributes to around 80% of all occupational diseases in operators [13]. Furthermore, when water-mixed fluids come into contact with the operator's skin, they usually cause irritation and allergic contact dermatitis [14,15]. Also, they possess poor biodegradability and thus may pollute the environment [16]. Tavella et al. indicated that the extraction of mineral oils during the refining of fossil fuel products results in land degradation and air pollution due to the release of toxic volatile organic compounds and greenhouse gases [17].

Extensive attempts by tribologists and scientists focused on replacing synthetic and harmful cutting fluids with eco-friendly and sustainable types using plant-based oils [18]. Unlike mineral-based cutting fluids, vegetable oils consist of triglycerides, which are esters derived from glycerol molecules interconnected with three fatty acids via long chains. Although their composition varies depending on the plant source, the main components of vegetable oils include saturated, monounsaturated, and polyunsaturated fatty acids. This is reflected in their physical and tribological properties, including their excellent biodegradability and non-toxicity properties. The mono- and polyunsaturated fatty acids produce stable lubricant films in the boundary lubrication zone due to the long polar fatty acid chains, thus increasing extreme pressure properties and decreasing friction and wear [19,20]. Additionally, vegetable oils possess a higher flash point while providing stable, adequate viscosities due to their strong intermolecular forces and high molecular weight, i.e., large molecules with long hydrocarbon chains [21].

Vegetable oils, extracted from a widespread array of botanical sources, exhibit a remarkably diverse spectrum of chemical compositions—particularly in terms of their fatty acid profiles, viscosity, oxidative stability, and thermal behavior. This inherent variability, while a testament to the richness of nature, poses a significant challenge when engineering these oils for metal cutting operations [22]. The smallest differences in saturation levels, chain lengths, and the presence of minor constituents like antioxidants or phospholipids can dramatically influence performance outcomes such as lubrication efficiency, biodegradability, and thermal resilience. Hence, selecting the most suitable vegetable oil that fits every metalworking operation is impractical, and a complex balancing act demands a careful match between the oil's intrinsic properties and the operational objectives of the intended machining operation [23]. This complexity encouraged ongoing research into exploring and modifying different vegetable oils to unlock their full potential as sustainable alternatives to mineral-based lubricants. Pereira et al. [24] demonstrated that CryoMQL (cryogenic CO_2 + MQL) outperforms standalone MQL in milling AISI 1045 steel, reducing tool wear by 30% and enabling 18% higher cutting speeds without increasing energy consumption. CryoMQL was also found to minimize adhesion, improving tool stability. This hybrid technique offers a viable eco-friendly alternative for industrial machining, reducing costs and environmental impacts compared to conventional methods. Shankar et al. [25] investigated the milling of a 7075–T6 hybrid aluminum metal matrix composite using some vegetable oils (palm, coconut, sunflower, and soya bean oils) against a commercial cutting fluid as a benchmark. The results showed that palm oil-based cutting fluid showed enhanced results for the minimum cutting force with minimal vibrations in comparison with other tested oils. Pereira et al. [26] conducted experiments on biodegradable oils (ECO-350, canola, sunflower) during the machining of Inconel 718, revealing that lower viscosity and increased friction enhance tool longevity. ECO-350 surpassed canola oil by 30%, whereas high-oleic sunflower oil extended tool life by 15% while maintaining a comparable ecological impact. These outcomes underscore the availability of sustainable, high-performance substitutes for conventional lubricants. Winter et al. [27] experimentally proved that jatropha oil offers better ecological benefits over mineral oils, while its success hinges on standardizing production practices to improve sustainability and economic viability without compromising food production. Minimum-quantity lubrication (MQL) is an eco-friendly machining technique that uses atomized biodegradable oil (10–100 mL/h) to reduce friction, heat, and lubricant consumption by up to 1000 times [28]. It enhances tool life and efficiency while eliminating toxicity risks compared to flood lubrication. The method delivers fine oil mist via pressurized air, ensuring effective lubrication in confined machining zones. Machining heat-resistant superalloys (HRSAs) requires precise cooling to preserve tool life. Accordingly, Pereira et al. [29] combined cryogenic CO2 cooling with MQL, achieving 3200 mm machined length—just 16% less than wet machining but more sustainable. While wet machining remains most effective, CryoMQL offers a stronger balance of performance and efficiency. López de Lacalle et al. [30] demonstrated that MQL reduces tool wear by over 30% compared to conventional emulsion coolants in the high-speed milling of aluminum alloys, achieving efficient cooling and lubrication with precise oil mist penetration. Their experiments showed that optimal nozzle positioning (135° to feed direction) and minimal oil use (0.04 cm^3/min) reduced cutting fluid consumption by 95% while maintaining performance. The findings of the study confirm MQL's dual advantages, which are significant cost savings and reduced environmental impact in industrial machining. Farfan-Cabrera et al. [31] developed biodegradable water-based lubricants using nopal cactus mucilage, showing that a 6.85 mg/mL mucilage solution reduced friction by 40% and wear by 35% compared to water in extreme pressure tests, matching the performance of commercial semisynthetic oil. The viscoelastic solution lowered cutting

forces by 22% versus dry machining and improved surface finish by 35% in turning tests, while remaining stable below 100 °C. This eco-friendly alternative cuts production costs by 88% per liter compared to conventional metalworking fluids, offering a sustainable solution for green manufacturing. Elbadawy et al. [32] investigated the use of cactus oil as an eco-friendly cutting fluid in machining 42CrMo4 steel under minimum-quantity lubrication (MQL). Compared to dry conditions, cactus oil improves surface roughness by 28% and reduces tool wear by 16% at a cutting depth of 1 mm. Additionally, compared to soluble oil, cactus oil enhanced surface roughness by 13% and reduced tool wear by 9%, highlighting its potential as a sustainable alternative for machining applications.

Cactus seed oil, belonging to Cactaceae, is well-adapted to dry regions, making cacti ideal for cultivation in drought-prone areas, poor or degraded soils, high temperatures, and low water availability [33]. This resilience not only reduces irrigation demands but also makes cactus oil a sustainable option that does not compete with food crops for fertile land. Furthermore, its adaptability to harsh climates further enhances its value as a sustainable, low-impact alternative to conventional mineral oils [34].

Cactus oil's high unsaturated fatty acid content makes it a promising bio-lubricant due to its good viscosity, high lubricity, and environmental performance [35]. The extracted oil is rich in unsaturated fatty acids, with linoleic acid (C18:2) ranging around 66% and oleic acid (C18:1) comprising up to 15%. Saturated fatty acids are present in smaller quantities, notably palmitic acid (C16:0) at about 12.7% and stearic acid (C18:0) at around 3.36% [36]. Thermally, it has a flash point approximately between 170 °C and 200 °C, indicating its stability under moderate heat. Though unsaturated fats can oxidize faster than saturated ones, cactus oil is also rich in natural antioxidants like tocopherols, which help protect against degradation [37].

However, the significant content of unsaturated acids presents limitations of low viscosity index, insufficient load-carrying capacity, and acid value variability based on the geographic location of plants [38,39]. These issues limit the consideration of cactus oil for industrial lubrication as a metalworking fluid.

Additives are, therefore, key components in base oils that enhance lubricant oil properties in terms of antioxidants, extreme pressure, and viscosity at elevated temperatures [40]. Recently, nano-additives such as zinc oxide (ZnO) [41], activated carbon nanoparticles (ACNPs) [42], graphene nanoplatelets [43], and molybdenum disulfide (MoS2) [44] in the form of nanoparticles, nanofibers, nanotubes, nanowires, nanorods, and nanosheets dispersed in base oil are a new class of cutting fluids called "nanofluids" [45,46]. A review conducted by Syahir et al. [47] concluded that vegetable oils may well replace mineral lubricants once their properties are augmented by proper nano-additive packages. Six empirically examined types of nanofluid (Al_2O_3, SiO_2, MoS_2, CNTs, SiC, and graphite) were dispersed in cottonseed oil for the milling of titanium alloy Ti-6Al-4V [48]. The nanofluids with Al_2O_3 showed minimal cutting forces and surface roughness, followed by SiO_2 nanoparticles. Talib et al. applied activated carbon nanoparticles (ACNPs) to enhance the lubricating performance of jatropha oil [42]. Another approach was tested by Nassef et al. [49] to harness the benefits of individual nanomaterials from graphene and ZnO by blending them with ionic liquid (IL) in rapeseed oil. The results showed enhancement in wettability and wear volume by around 60% and 80%, respectively, in comparison with benchmark metalworking fluids. Talib et al. [50] demonstrated that adding 0.05 wt.% hexagonal boron nitride (hBN) nanoparticles to modified jatropha oil (MJO) boosted its viscosity index by 7% over pure MJO and 52% over synthetic esters. This nano-enhanced lubricant formed a superior protective film, reducing the cutting temperature by 5% and cutting force by 9% compared to synthetic esters during turning. Mushtaq et al. [51] explored the impact of adding graphene nanoflakes (0.3%, 0.5%, 0.7%) to jatropha oil, testing tribological

performance under varying loads and speeds. The results showed that 0.5% graphene reduced the coefficient of friction by 44% and wear by 43.7% compared to pure jatropha oil. The previous research works demonstrate the significant potential of nanomaterials in enhancing lubricant performance.

Since nano-additives are present in small concentrations in the cutting fluids, the applied lubrication methodology must ensure that they are delivered directly at the tool–workpiece interface, maximizing their lubricating and heat-reducing effects. Conventional flood lubrication disperses the fluid across a broader area, leading to the dilution of additives and less effective interaction with the cutting zone. Hence, minimum-quantity lubrication (MQL) has been promoted over the last decade due to its superior results [52]. This technique is based on mixing minimum-quantity lubricants with high-pressure air; in addition, the high-pressure air plays a role in cooling and chip removal [53]. MQL, flood, and dry machining conditions were investigated in the milling of aluminum. It was reported that MQL produces better product quality in comparison to traditional machining [54]. Many studies have investigated the effectiveness of nanofluids and MQL integration in turning, grinding, and milling. It was found that when nano-additives of various sizes are suspended in a base oil, the heat transfer coefficient is increased so that the cutting zone's heat is uniformly distributed [55–57]. Thakur et al. [58] investigated the effectiveness of different cooling–lubrication techniques, including dry machining, conventional wet cooling, and nanofluid-assisted minimum-quantity lubrication (MQL), in improving machining performance when turning EN-24 alloy steel. The results demonstrated that using hybrid Al–CuO nanofluid MQL leads to superior surface finish, lower cutting temperatures, and reduced tool forces compared to traditional methods. Nanofluid MQL using graphene as a nano-additive was applied in the machining of Ti–6Al–4 alloy to investigate its influence on the machining parameters [59]. The values of cutting forces, tool wear, and surface roughness were then compared with those obtained in the case of dry machining, and nanofluid MQL demonstrated minimal cutting forces and superior surface finish.

The previous review of the literature reveals substantial research endeavors aimed at replacing conventional mineral oil-based cutting fluids with vegetable oil alternatives in machining operations, primarily to address growing environmental and health concerns. Concurrently, the advances in nanotechnology have promoted investigations into the integration of carbonaceous and metallic nano-additives into base fluids to enhance their lubricating performance. Despite this progress, the predominant reliance on food-grade vegetable oils remains, which raises arguments about cost, supply chain sustainability, and competition with food production.

In response to this challenge, the present study proposes a novel, eco-friendly cutting fluid formulated from non-edible cactus oil, thereby offering a sustainable and underutilized alternative with minimal agricultural conflict. To improve its inherent limitations in load-carrying capacity and wear resistance, cactus oil was functionalized with activated carbon nanoparticles (ACNPs) at concentrations of 0.025 wt.%, 0.05 wt.%, and 0.1 wt.%. Given the complex nature of machining processes, where tool–workpiece interactions, strain rates, cutting geometry, and thermal gradients critically influence outcomes, a detailed investigation was conducted to characterize the physical, chemical, rheological, and tribological properties of the developed nanofluids. This study adopts two lubrication modes, dry cutting and minimum-quantity lubrication (MQL), to evaluate the machining performance during the turning of H13 steel. This work benchmarks the proposed green formulations against two commercially available cutting fluids.

2. Materials and Methods

2.1. Nano-Additive Synthesis and Characterization

Activated carbon nanoparticles (ACNPs) are derived in this work from processing polymeric polyethylene terephthalate (PET) waste [60]. A 25 g portion of the shredded PET was placed in a sealed stainless steel autoclave and heated in an electric muffle furnace (ASH AMF 25N, Across International, Livingston, CA, USA) at a rate of 25 °C per minute up to 500 °C for one hour. The system was then allowed to cool for about 12 h. The resulting synthetic AC was ground using an Electric Grain Spices Multifunctional grinder (ST3-E4842UK, STX International, UK) for 10 min to achieve particle sizes below 0.09 µm.

The purity of AC is mainly dependent on the material type of plastic waste and the pyrolysis process itself [61]. Hence, a scanning electron microscope (SEM) (JEOL JSM-IT200, JEOL Ltd., Tokyo, Japan) and transmission electron microscope (TEM) (JEOL JEM-2100, JOEL Ltd., Tokyo, Japan) were used to evaluate the structural properties, particle size, and morphology of the synthesized ACNPs. Moreover, the analysis of microstructural phases and the degree of crystallinity was carried out through the examination of characteristic peaks of AC powder using X-ray diffraction (XRD) spectroscopy (Empyrean Malvern Panalytical, Almelo City, The Netherlands). XRD patterns are acquired at 40 keV and 30 mA utilizing Cu-Kα1 radiation. To assess the quality of the nanostructure, the functional groups of AC composition were investigated using the Bruker Vertex 70 Fourier-transform infrared (FTIR) spectroscope (Bruker Company, Billerica, MA, USA) with a detection range spanning from 400 to 4000 cm^{-1}. The structural flaws of AC were attained via Raman spectroscopy (WITec alpha 300 R, WITec Wissenschaftliche Instrumente und Technologie GmbH, ULM, Germany). The examination commenced by subjecting the rGO specimen to 3 mW power with an applied laser wavelength of 532 nm. Subsequently, the ultimate spectrum was recorded and exhibited within a 20 s detection period. Brunauer–Emmett–Teller (BET) at −200 °C (Belsorbmini II, BEl Inc., Osaka, Japan) was applied to obtain an estimation of the surface area of the ACNPs.

2.2. Cutting Fluid Sample Preparation

Samples of cactus oil in its plain form and blended with three different concentrations of ACNPs (0.025 wt.%, 0.05 wt.%, and 0.1 wt.% ACNPs) were prepared, as shown in Table 1. The selected concentrations of ACNPs were guided by considering the reported research works in the literature [42]. Blends of oil samples with ACNPs were first weighed using a commercial scale (Mettler-Toledo GmbH, Greifensee, Germany), and then, they were mixed using a magnetic stirrer at 700 rpm for 30 min to prevent agglomeration. As a benchmark, mineral-based oil was procured from the local market and emulsified by diluting it with water at a ratio of 1:9. Figure 1 shows the prepared bio-oil samples along with the mineral oil-based emulsion (soluble oil).

Table 1. Designations of prepared cutting fluid samples.

Cutting Fluid Type	Sample	ACNP Concentration
Cactus oil	CO	-
	CO1	0.025 wt.%
	CO2	0.05 wt.%
	CO3	0.1 wt.%
Mineral oil-based emulsion lubricant	SO	-

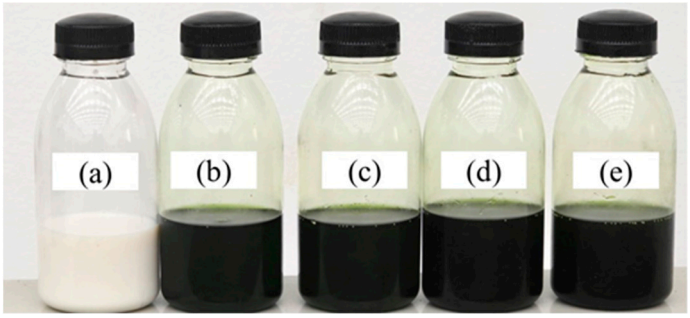


Figure 1. Prepared oil samples: (**a**) soluble oil, (**b**) cactus oil in its plain form, (**c**) cactus oil with 0.025 wt.% ACNPs, (**d**) cactus oil with 0.05 wt.% ACNPs, and (**e**) cactus oil with 0.1 wt.% ACNPs.

2.3. Wettability Test

One crucial characteristic of an effective cutting fluid for reducing friction is wettability. Surface tension is the controlling factor of the contact angle (CA) and hence the wettability of the oil samples on the cutting tool surface. It is generated as a result of the surface molecules of the oil drop being pulled by cohesive forces inwards to the center, leading to a spherical shape with the minimum surface area possible. The wettability test of oil samples was conducted using a contact angle goniometer. During each test, a droplet of the cutting fluid was released from a syringe onto the steel work surface, while the monochrome CCD camera captured an image of the droplet. The image was then processed to calculate the CA using the associated software.

2.4. Flash Point Test

Flash point testing of oil blends was conducted to evaluate their flammability and safety during metal cutting operation. The Cleveland Open Cup (COC) was used to examine the flash point according to ASTM D92 [62]. During the test, an open metallic cup was filled with the cactus oil sample, and then, the cup was heated at a predetermined rate. An ignitor was moved over the cup surface in a frequent way until the vapor from oil flashed, and the corresponding temperature was recorded as the oil flash point.

2.5. Rheological Test

The rheological properties of cactus oil samples were evaluated using a rotational rheometer (Kinexus Prime lab +, Netzsch GmbH, Selb, Germany). Since most oils are classified as non-Newtonian, their dynamic viscosities are dependent on the shear rate. To investigate this relationship, the dynamic viscosity of each oil sample was determined according to ASTM D2196-20 [63]. In each test, 0.3 mL of an oil sample was subjected to a preselected range of shear rates from 0.1 to 100/s. This broad span of shear rate values provides a clear indication of the Newtonian behavior of oil samples. Since dynamic viscosity is a temperature-dependent property, tests were conducted on the samples at 40 °C and 100 °C to evaluate the behavior of cutting fluids at different operating temperatures. The Newtonian behavior of the test samples was determined via curve fitting of the obtained viscosity data using a power law model (Equation (1)) [49]. Each test was repeated three times to confirm the results' repeatability.

$$\eta = K \cdot \gamma^n \quad (1)$$

where η is the viscosity, γ is the shear rate, K is the consistency index, and n is the flow behavior index.

2.6. Tribological Test

A rheometer was used to determine the tribological properties of each oil sample in terms of the coefficient of friction (COF) according to ASTM D-4172 [64]. A sample of 0.11 mL of each tested oil was used to fill a cup with three pads, which represented the stationary lower part of the attachment, while a 316 stainless steel rotating ball of 12.7 mm diameter was used as the upper part, pressing against the pads at three points. The ball was driven to rotate against the pads at a specific range of angular velocities from 0.1 to 300 rad/s under 1 GPa pressure at 25 °C. The tests were conducted three times for each specimen to ensure high repeatability. The frictional torque was measured during each test, and its values in the boundary regime were used to calculate the coefficient of friction using Equation (2).

$$\mu = T\sqrt{\frac{6}{3Fr}} \tag{2}$$

where μ is the coefficient of friction, T is the frictional torque, F is the normal load, and r is the radius of the contact surface.

2.7. Metal Cutting Test

The objective of this section is to understand the combined effects of the proposed cutting fluids along with machining parameters on the workpiece surface roughness and the tool flank wear. For this purpose, the cutting tests were designed using the Taguchi L18 scheme. Machining performance during each test was investigated using the test setup, as shown in Figure 2.

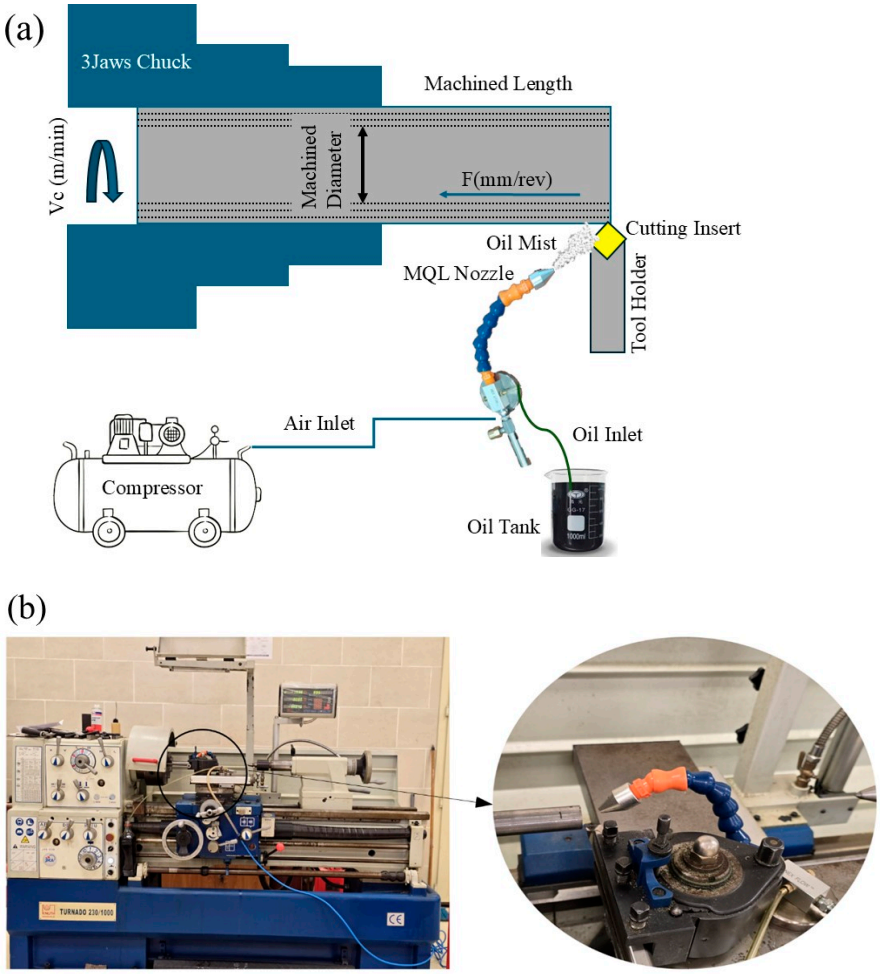


Figure 2. (**a**) Schematic drawing of the machining setup and (**b**) the used center lathe machine.

The details of the machining setup including tool material, workpiece material, and MQL settings in this study are presented in Table 2. A portable MQL system (NEX Flow) was attached to a center lathe (Turnado 230/1000, Kunth, Remscheid, Germany) to supply the developed cutting fluid at a pressure of 4 bar and a flow rate of 125 mL/hr into the cutting zone during the cutting tests. The MQL nozzle was positioned at a 45° angle relative to the tool face and maintained at a distance of 20 mm from the cutting edge, ensuring the precise delivery of the lubricant mist to the tool–chip interface. This configuration aligns with the study's findings of Talib et al. [50], who demonstrated that a moderate angle (45°) optimizes lubrication film formation, as evidenced by the reduced cutting force (383 N) and temperature (210 °C) when using MJO + 0.05 wt.% hBN nanolubricant. A 60° triangular cermet carbide (Tungaloy TPMT130304-24NS9530, Tungaloy Corporation, Iwaki, Fukushima, Japan) was utilized as the cutting insert. The workpiece material was H13 steel grade with a hardness of 30 RC, and dimensions of 30 mm in diameter and 60 mm in length. The chemical composition of workpieces was confirmed by spectroscopic analysis (SPECTROTEST TXC35). Three levels of the machining parameters were selected based on optimum cutting conditions from previous work. Tests under dry conditions and MQL using soluble oil as a conventional water-based cutting fluid were considered as benchmark lubrication methods, as shown in Table 3.

Table 2. Machining test setup parameters.

Setup Parameters	Description
Machine tool	Center lathe (Turnado 230/1000)
Workpiece	H13 steel (30 mm diameter)
Cutting tool	Cermet Carbide Insert (Tungaloy Tpmt130304- 24ns9530)
Cutting fluid System	MQL (NEX Flow)
Distance between the MQL nozzle and workpiece	20 mm
Flow rate under MQL	125 mL/h
The pressure of air under MQL	4-bar
MQL nozzle angle	45°

Table 3. Planned process parameters and their levels.

Process Parameter	Values					
Depth of cut d (mm)	0.3		0.4		0.5	
Feed rate f (mm/rev)	0.031		0.034		0.038	
Cutting speed N (rpm)	605		1330		2000	
Cutting fluid	Dry	Soluble Oil	Cactus Oil (CO)	Cactus Oil with 0.025 wt.% AC (CO1)	Cactus Oil with 0.05 wt.% AC (CO2)	Cactus Oil with 0.1 wt. % AC (CO3)

2.8. Workpiece Surface Roughness and Tool Flank Wear

The outcomes from the designed cutting tests were quantitatively evaluated in this work through the measurement of workpiece surface roughness and tool flank wear. After each cutting test, the workpiece was tested for surface roughness using a 3D laser microscope (KEYENCE, VK-X100 SERIES, Keyence corporation, Osaka, Japan) according to JIS B0601:2001(ISO 4287:1997 [65]). The value of the arithmetic mean surface roughness

(Ra) was determined by averaging three measurements taken from each machined surface in both the same and perpendicular orientations relative to the feed motion.

On the other hand, the cutting insert wear was evaluated by measuring the flank wear parameter (VBmax) as the maximum width of flank wear land measured according to ISO 3685 [66] using a tool maker microscope (Mitutoyo MF-A2010D MF Series 176 Measuring Microscope 176-862-10, Mitutoyo Corporation, Kawasaki, Kanagawa, Japan). The flank wear indicates the influence of the thermo-mechanical loads acting on the cutting tool during the turning operation. VBmax is determined as an average of three successive measurements.

3. Results and Discussion

3.1. ACNP Characterization Results

The SEM micrographs in Figure 3a at 1000× magnification reveal aggregated ACNPs with irregular blocky morphologies. The particles exhibit smooth surfaces and varying sizes. During the analysis of AC nanopowder via SEM, particle agglomeration and charging effects can distort size measurements. To mitigate this effect, nanoparticles are often dispersed in isopropanol and imaged using SEM at a 50,000× magnification level (Figure 3b). The average particle diameter is around 26.5 nm, indicative of continuous material consumption during activation. XRD analysis confirms a high carbon content of 97.56 wt.% with trace oxygen (2.44 wt.%), reflecting the material's purity.

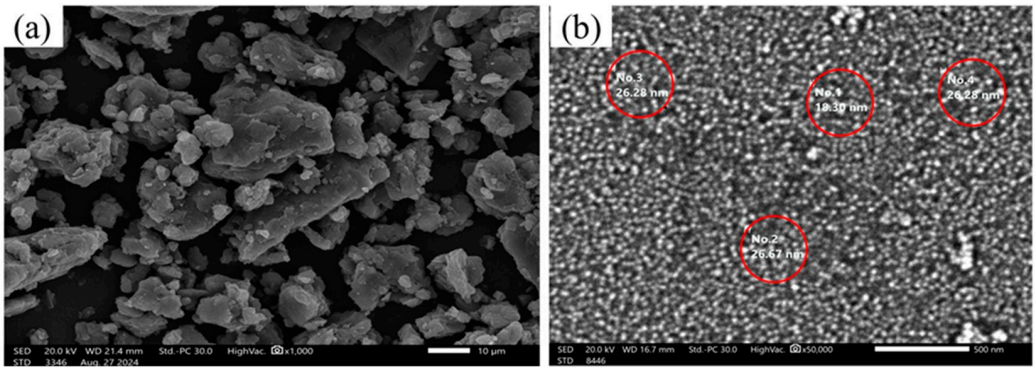


Figure 3. (**a**) SEM micrograph and (**b**) liquid-phase SEM micrograph of ACNPs.

The BET analysis (Table 4) demonstrates a microporous structure with a surface area of 448.88 m^2/g, a pore volume of 0.2029 cm^3/g, and an average pore diameter of 1.808 nm. The high porosity arises from hydrocarbon radical interactions during pyrolysis, yielding an amorphous, high-surface-area material.

Table 4. BET surface area, total pore volume, and mean pore diameter of AC nanopowder.

Sample	BET Surface Area (m^2 g^{-1})	Total Pore Volume (cm^3 g^{-1})	Mean Pore Diameter (nm)
AC	448.88	0.2029	1.808

The XRD patterns (Figure 4a) show broad peaks at 2θ ≈ 21–23° (002 plane) and 43.2° (101 plane), confirming the amorphous nature of AC derived from PET waste. Raman spectroscopy (Figure 4b) further validates the structure with distinct D (1348 cm^{-1}) and G (1590 cm^{-1}) bands, signifying lattice defects and C=C stretching, respectively. Minor 2D (2680 cm^{-1}) and S3 (2844 cm^{-1}) bands suggest few-layered carbon domains. FTIR spectra (Figure 5) reveal key functional groups. The peak at 3421.62 cm^{-1} confirms the presence of O–H stretching (hydrogen-bonded alcohols/phenols), while the peak at 1572.49 cm^{-1} belongs to the C=C aromatic ring vibrations. The other peaks at 1177.33 cm^{-1}

and 506.27 cm^{-1} are indicative of C–O stretching and aromatic ring deformations, corroborating the carbonaceous structure.

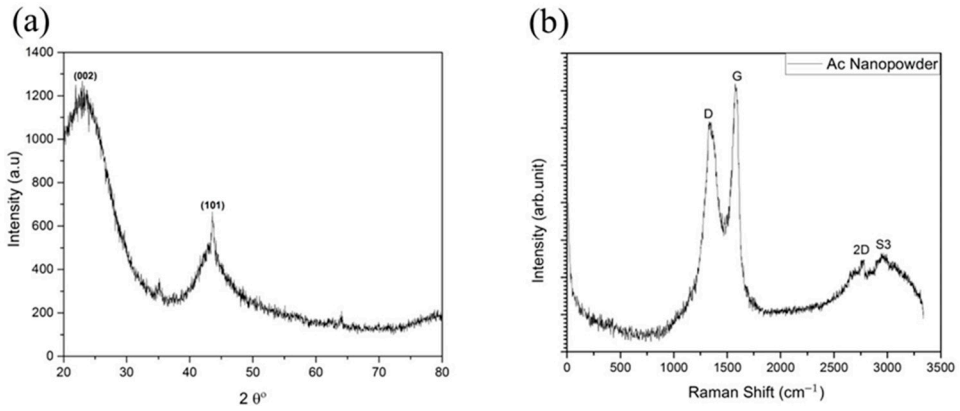


Figure 4. (**a**) XRD pattern and (**b**) Raman spectrum of the synthesized ACNPs.

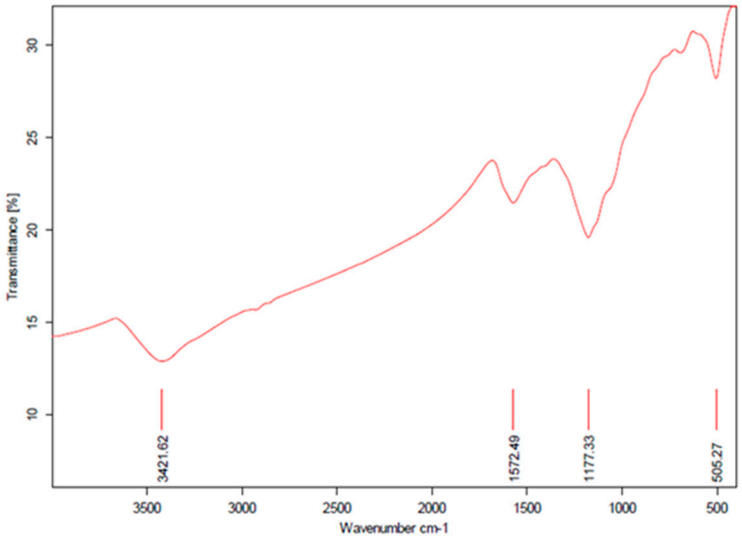


Figure 5. FTIR spectrum of the synthesized ACNPs.

3.2. Physical–Chemical Results

The predominant fatty acids found in cactus oil are poly- and monounsaturated fatty acids, summing up to 80%. This includes linoleic acid (C18:2) with an amount of 66%, oleic acid (C18:1), and other minor saturated fatty acids such as 15% palmitic acid (C16:0) with 12.7%, which are consistent with the findings in [36,67,68]. Although the large presence of the unsaturated fatty acids enhances the pour point, it harms the thermal and oxidation stabilities of cactus oil. However, cactus seed oil contains unique natural antioxidants that delay lipid peroxidation and enhance oxidative stability, such as tocopherols and phenolic compounds.

In return, kinematic viscosity is affected by the chain length of fatty acids and the degree of unsaturation. While the amount of unsaturated fatty acids decreases the viscosity level, the longer chain length plays an important role in keeping the viscosity values at elevated levels [37,69].

The kinematic viscosity values at 40 °C and at 100 °C of the CO samples (in their plain form) are found to be 85 and 21.75 cSt, which are higher by 118% and 117.5% than those of the SO samples, respectively, as shown in Table 5. This may be justified by the presence of the large molecular structure of the longer carbon chains in fatty acids (C16–C18), creating a thicker film between the rubbing contacts [38]. In comparison with soluble oil (SO),

Vasco 6000, and Zubora 67H from a review of the literature [49], cactus oil possesses higher kinematic viscosity at 40 °C by around two folds.

Table 5. Physical properties of cactus oil in comparison with soluble oil and benchmark cutting fluids from a review of the literature.

Samples	Cactus Oil	Soluble Oil	Blaser Vasco 6000 [49]	Zubora 67H [49]
Kinematic viscosity at 40 °C (cSt)	85	39	42	40
Kinematic viscosity at 100 °C (cSt)	21.75	10	10.3	9
Viscosity index	283.21	260.012	213	216
Density (gm/cm^3)	0.9194	0.9898	0.99	0.9898
Flash point (°C)	212	168	129	168
PH value	5.14	9.50	-	9.50
Chemical structure	Linoleic acid (C18:2), oleic acid (C18:1), palmitic acid (C:16:0)	Water emulsion (10% oil + 90% water)	Water-miscible, ester oil base, boron, formaldehyde, and chlorine-free	

By observing the viscosity index (VI) values, cactus oil is found to have a VI of 283.21, which is 9% higher than that of the commercial soluble oil. The VI of cactus oil was also found to be better than Blaser Vasco 6000 and Zubora 67H, indicating excellent viscosity stability at elevated temperatures. This is especially valuable in the context of metal cutting applications that require a reliable kinematic viscosity of lubricants, thus guaranteeing the formation of a stable tribofilm across an extended range of operating temperatures.

3.3. Wettability Results

The molecular structure and nano-additives are two factors that define the surface tension of the oil. Figures 6 and 7 show the measured CA of cactus oil samples as well as the soluble oil. It is observed that the recovered CA decreases gradually over the test time until it reaches a steady state after 4 s. Plain cactus oil reached a contact angle of 25.81°, while the soluble oil exhibited the largest CA value of around 39.24°. The addition of ACNPs at different blends to the cactus oil enhanced the physical adsorption between the oil and the contact surface. In the case of the CO2 sample, the CA was improved by up to 40% and 60% in comparison with CO and commercial SO, respectively. The wettability results of Vasco 6000 and Zubora 67H from a previous investigation [49] are used for comparison. Both emulsions showed good droplet dispersion over the surface, exhibited by contact angles of 27° and 14°, respectively, which is attributed to their chemical composition such as carboxylic acid and alkanolamides to enhance the dispersal of oil in water. The results in general indicate comparable wettability of cactus oil blends with ACNPs to Zubora 67H and Vasco 6000 oils [49], i.e., effective spreading of cutting fluid is attainable in the secondary shear zone during cutting operation.

The variation in CA results amongst samples is largely explained by the contribution of the fluid's chemical composition and the presence of ACNPs in the fluid. Cactus oil possesses long hydrocarbon chains of linoleic acid (C18:2), oleic acid (C18:1), and palmitic acid (C:16:0), which tend to create intermolecular forces between the oil molecules and steel surface. The double bond presented in polyunsaturated fatty acids contributes to their intermolecular forces that overcome the surface tension and reduce CA. Lundgren et al. [70]

explained that linoleic and oleic acids adsorb well on steel surfaces, with linoleic acids tending to form multilayers. Chemically adsorbed quantities of fatty acids were found due to interactions between the carboxylic head groups and adsorption sites at the surface, while physically adsorbed layers were attributed to the presence of unsaturated fatty acids. The addition of ACNPs at low concentrations to cactus oil further decreased the surface tension (cactus oil with 0.05 wt.% AC (CO2) followed by cactus oil with 0.025 wt.% AC (CO1), then followed by the worst case of cactus oil with 0.1 wt.% AC (CO3)). This can be justified by the possible aggregation of nanoparticles in the oil drop, which increased the surface tension and reduced the spread of the oil droplet on the steel surface. While cactus oil predominantly contains monounsaturated fatty acids showing lower polarity, i.e., lower adsorption to the surface, ACNPs enhance the adsorption properties of cactus oil. From FTIR analysis, ACNPs possess polar functional groups such as hydroxyl (-OH), carboxyl (-COOH), or amino (-NH) groups. They are well known for their high adsorption properties of heavy metals in water treatment [60,71]. Furthermore, ACNPs proved to form a stable tribofilm layer on the steel surface when tested in the four-ball wear test and examined by SEM EDX due to the polar characteristics of their functional groups [72].

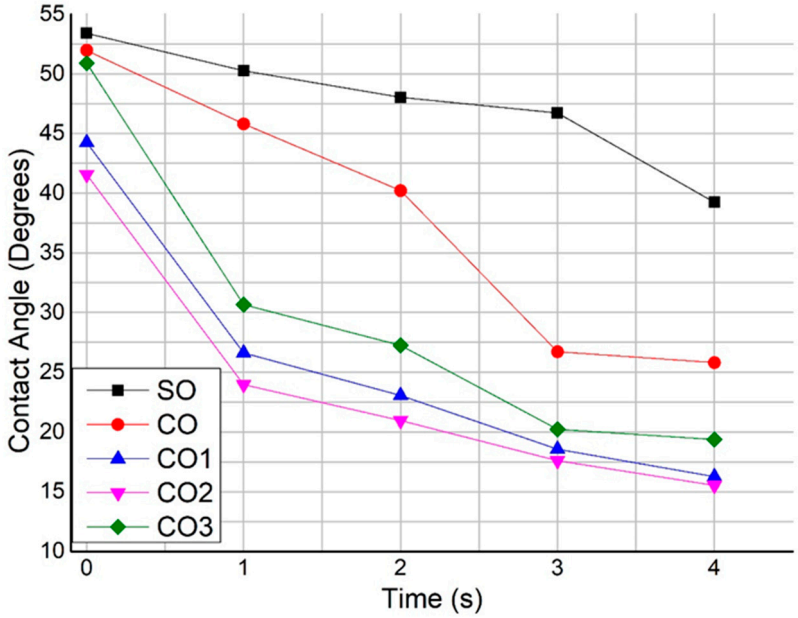


Figure 6. Measured contact angle on H13 steel substrate plate over time.

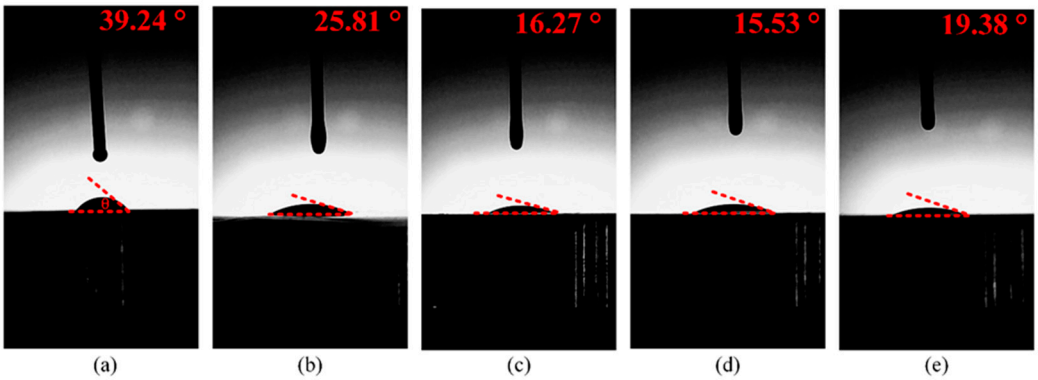


Figure 7. The interactions between droplets of cutting fluid and the H13 steel plate after 4s: (**a**) soluble oil (SO), (**b**) plain cactus oil (CO), (**c**) cactus oil with 0.025 wt.% AC (CO1), (**d**) cactus oil with 0.05 wt.% AC (CO2), and (**e**) cactus oil with 0.1 wt.% AC (CO3).

3.4. Rheological Results

Figure 8 shows the shear rate–dynamic viscosity patterns for each cactus oil sample at both 40 °C and 100 °C recorded at shear rates ranging from 0.1 s^{-1} to 100 s^{-1}. The results confirm Newtonian behavior in the case of the CO sample, i.e., it experiences a constant viscosity value along the entire tested shear rate range. This is also indicated by checking the flow behavior index n value in the power law model, which is found to be around 1.04, especially at low shear rates. The n value remained almost the same (1.076) at elevated temperatures, confirming a stable and constant dynamic viscosity.

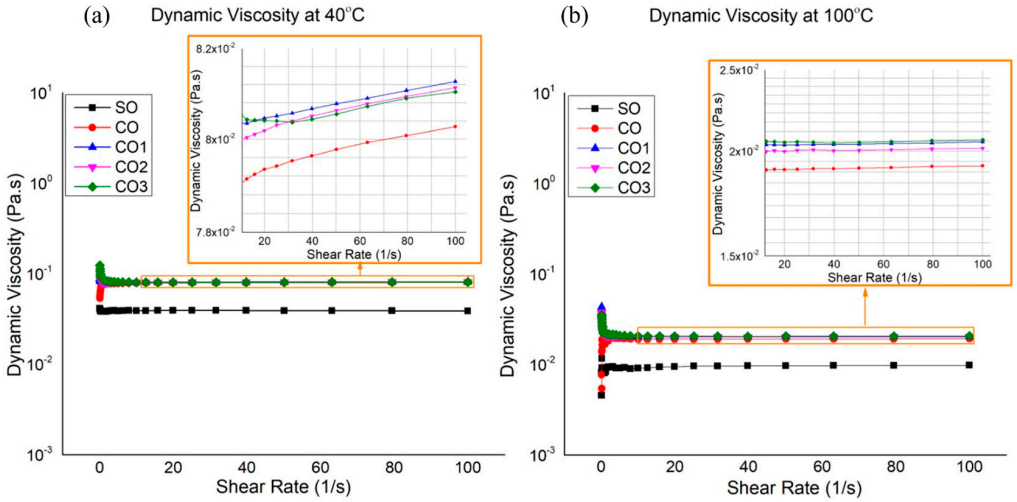


Figure 8. Dynamic viscosity and shear rate for the cutting fluid samples at (**a**) 40 °C and (**b**) 100 °C.

In comparison, the average dynamic viscosities of CO samples are found to be 100% higher than those of SO at both temperatures. The introduction of ACNPs to cactus oil increased its dynamic viscosity at 40 °C from 9% to 15% compared to the CO sample. At higher shear rates (10–100 s^{-1}), the presence of ACNPs in cactus oil led to a slight decrease in shear viscosity, indicated by a lower exponent n value (0.955) for higher concentrations of ACNPs in samples CO2 and CO3. This means that slight shear thinning behavior took place with increasing shear rate, indicating a reduction in viscosity and more flowability at higher velocities. The flow of oil during higher shear rates enables the ACNPs suspended in the oil to rearrange themselves and align with the oil layers in the direction of flow [73,74]. As the ACNP content increased, the material exhibited more pronounced shear thinning, an effect attributed to nanoparticle agglomeration that is disrupted under shear, breaking up the clusters and thus facilitating flow [75].

An increase in viscosity could, in some cases, hinder fluid penetration into the cutting zone. However, the viscosity increase due to ACNP addition was found to be moderate (9–15% at 40 °C). This slight increase contributed to better thermal stability and reduced shear thinning at elevated temperatures, an important feature for maintaining film integrity in high-pressure and high-temperature conditions. Furthermore, under the high coolant pressures typical of the cutting zone, the fluid is forcibly injected into the tool–chip interface under the MQL system, which may mitigate the potential negative impact of increased viscosity.

3.5. Tribological Results

Figure 9 illustrates the frictional performance of the prepared samples in comparison to SO. The SO sample exhibited superior behavior at lower sliding speeds, displaying lower coefficients of friction (COFs); however, it showed a steadily increasing trend with rising speed. At a threshold speed of 0.01 m/s, SO recorded the highest COF among all

tested samples. In contrast, the cactus-based samples demonstrated more stable frictional behavior, characterized by smooth, consistent curves. Notably, the CO samples mixed with ACNPs exhibited comparable friction values.

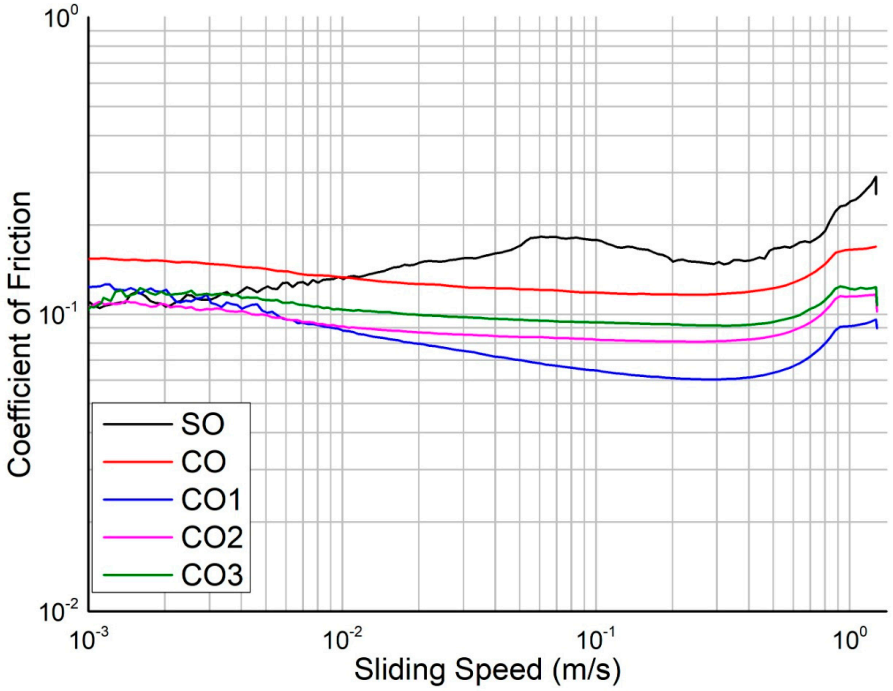


Figure 9. Stribeck curves for the prepared samples at 25 °C.

The CO2 sample achieved a significant reduction in friction, approximately 32% compared to CO, although its COF remained similar to that of SO up to a speed of 2×10^{-3} m/s. From 6×10^{-3} m/s onward, the CO1 sample began to exhibit a decreasing trend in COF, indicating a transition from the boundary to the mixed lubrication regime and resulting in the lowest friction values observed. An earlier transition from boundary to mixed lubrication was also noted in the CO samples compared to SO.

In order to discuss the frictional results, it is essential to consider the chemical structure of cactus oil. Three main acids in cactus oil contribute to the formation of a stable lubricant film between the rubbing contact, namely linoleic acid, oleic acid, and palmitic acid [36]. This result is in accordance with [76], which added cactus oil to mineral lubricant. The study demonstrated that the frictional performance of cactus oil was improved due to the long fatty acid chains in cactus oil after testing in the four-ball wear test, especially the mixture containing 20–80% cactus–mineral mixture. Further explanation of the tribological mechanism of both the base bio-oil and the ACNPs will be discussed in the tool wear part.

3.6. Metal Cutting Results

a. Workpiece surface roughness

The surface roughness of H13 steel under varying lubrication conditions and machining parameters is summarized in Table 6 and Figure 10. Key findings are supported by the scanned surface topographies using a 3D laser microscope, as shown in Figure 11. The surface roughness showed its highest values in the case of dry lubrication, peaking at 4.09 µm in extreme operating conditions with a mean value of 2.8 µm (Figure 10). This is due to the intense generated friction and corresponding elevated temperatures at the tool/workpiece interface. This result is further confirmed by observing the surface roughness image of the machine surface in Figure 11a. High friction and localized heat generation led to plastic deformation, which conforms with the findings of [77].

Table 6. Results of average surface roughness values (μm) under effect of selected design-of-experiment parameters.

Cutting Fluid	Speed (rpm)	Depth of Cut (mm)	Feed (mm/rev)	Average Surface Roughness (Vertical) (μm)	Average Surface Roughness (Horizontal) (μm)	Average Surface Roughness (Vertical + Horizontal) (μm)
Dry	605	0.3	0.031	2.00	2.18	2.09
Dry	1330	0.4	0.034	2.10	2.26	2.18
Dry	2000	0.5	0.038	4.27	3.91	4.09
SO	605	0.3	0.034	2.99	2.52	2.76
SO	1330	0.4	0.038	2.57	2.19	2.38
SO	2000	0.5	0.031	1.91	2.04	1.98
CO	605	0.4	0.031	2.58	2.43	2.50
CO	1330	0.5	0.034	2.40	1.97	2.19
CO	2000	0.3	0.038	1.93	1.66	1.80
CO1	605	0.5	0.038	2.49	2.03	2.26
CO1	1330	0.3	0.031	2.18	1.88	2.03
CO1	2000	0.4	0.034	2.18	1.67	1.92
CO2	605	0.4	0.038	2.16	2.13	2.15
CO2	1330	0.5	0.031	2.07	1.28	1.68
CO2	2000	0.3	0.034	2.03	1.18	1.60
CO3	605	0.5	0.034	2.20	1.91	2.06
CO3	1330	0.3	0.038	2.18	1.61	1.90
CO3	2000	0.4	0.031	2.13	1.55	1.84

According to the main effects plot for means (Figure 10), the application of SO reduced the mean surface roughness by 15% compared to dry machining. The surface roughness in the case of SO ranges between 1.98 and 2.76 μm, as shown in Table 6. The optimum conditions that achieved the lowest roughness were found at 2000 rpm, 0.5 mm depth, and 0.031 mm/rev feed. SO's emulsion properties improved cooling and chip evacuation, reducing the severity of BUE and abrasive wear mechanisms. However, its performance lagged behind cactus oil blends due to inferior boundary lubrication from mineral oil's shorter hydrocarbon chains, which provide weaker adsorption on metal surfaces compared to the long-chain fatty acids in vegetable oils [25]. This is shown in Figure 11b by the presence of deeper feed marks and tearing marks due to insufficient lubrication.

The use of plain cactus oil (CO) as a cutting fluid significantly improved the surface finish compared to SO lubrication and dry machining, exhibiting a 9% and 22.5% reduction in the surface roughness, respectively (Figure 10). This improvement is attributed to the high concentration of unsaturated fatty acids (66% linoleic acid, 15% oleic acid) in cactus oil, which form strong adsorbed lubrication films on the workpiece surface. The long hydrocarbon chains of these fatty acids enhance boundary lubrication, reducing metal-to-metal contact and minimizing adhesive wear. Additionally, the Newtonian behavior of CO (discussed in Section 3.4) ensures stable viscosity under varying shear rates, maintaining a consistent lubricating film even at high cutting speeds. The reduction in surface roughness aligns with findings by Lundgren et al. [70], who demonstrated that unsaturated fatty acids like linoleic acid effectively reduce friction through chemisorption on steel surfaces.



Figure 10. Main effects plot for means for surface roughness value (µm).

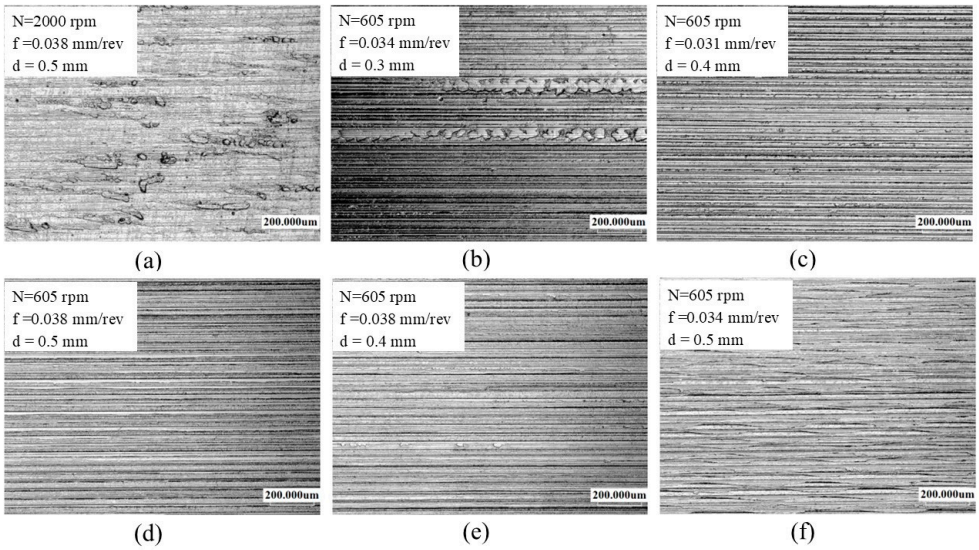


Figure 11. Machined surfaces of the workpieces using the tested lubricants and lubrication techniques: (**a**) dry lubrication, (**b**) soluble oil (SO), (**c**) plain cactus oil (CO), (**d**) cactus oil with 0.025 wt.% AC (CO1), (**e**) cactus oil with 0.05 wt.% AC (CO2), and (**f**) cactus oil with 0.1 wt.% AC (CO3).

The incorporation of activated carbon nanoparticles (ACNPs) further enhanced the tribological performance of cactus oil, with CO2 (0.05 wt.% ACNPs) achieving 23.6% improvement over soluble oil (SO) and 35% better than dry lubrication. Figure 11d–f show shallow grooves with the absence of micro-pits, indicating low friction and localized heat on the workpiece surface. The microporous structure of ACNPs with a large surface area forms a durable tribofilm, mitigating the friction between the tool and workpiece. The polar functional groups (e.g., C–O, O–H) identified via FTIR further enhanced surface adhesion, similar to graphene-enhanced lubricants [59].

At higher ACNP concentrations (CO3), roughness slightly increased to be between 1.84 and 2.06 µm, as shown in Figure 11f. This may be attributed to nanoparticle agglomeration, which disrupted the uniform film formation and induced harmful abrasive wear, where excessive additive loading led to inhomogeneous nanoparticle dispersion and worse workpiece surface quality.

The influence of machining parameters on surface roughness followed predictable yet nuanced trends across all lubrication conditions. Cutting speed exhibited a considerable effect on surface quality, with optimal results occurring at 2000 rpm (Ra = 1.60 µm for CO2). At lower speeds (605 rpm), insufficient thermal softening of the workpiece material promoted built-up edge formation, increasing roughness by 18–22% [5]. Conversely, excessive speeds (2000 rpm) generated elevated cutting temperatures that accelerated tool wear, particularly under dry conditions where roughness values spiked to 4.09 µm [6]. This trend aligns with the findings of [48] in their study of H13 steel machining.

Feed rate demonstrated a more direct correlation with surface finish, where increasing from 0.031 to 0.038 mm/rev consistently raised roughness by 15–20% across all lubricants (Table 6). The higher feed rates produced thicker chips that exerted greater normal forces on the tool flank, exacerbating surface ploughing effects [54]. The depth of cut impacts was most pronounced at extreme values. Shallow cuts (0.3 mm) produced the best surface finish (Ra = 1.60 µm for CO2) by minimizing tool deflection and vibration [4], while deeper cuts (0.5 mm) increased roughness by 25–30% through heightened mechanical loads. Hence, the optimum machining conditions that achieved the lowest roughness (1.60 µm) in the case of cactus oil blends (CO2) were found at 2000 rpm, 0.3 mm depth, and 0.034 mm/rev feed.

b. Tool Flank Wear

Table 7 and Figure 12 summarize the flank wear results, while Figure 13 illustrates the wear profiles obtained via SEM/EDX. The flank wear results demonstrate significant variations across lubrication conditions, with clear trends emerging from the experimental data. Under dry machining conditions, the insert experienced a mean flank wear of 0.37 mm, reaching a maximum of 0.76 mm, as shown in Table 7, at the most aggressive cutting parameter combination in the design of experiments (2000 rpm, 0.5 mm depth of cut, 0.038 mm/rev feed). Adhesive wear is obviously witnessed in the SEM results, which occurred through localized welding and built-up edge formation. The wear mechanism is confirmed by EDX analysis, showing significant iron concentration transfer to the carbide insert surface, as shown in Figure 13b.

Table 7. Results of average flank wear values under the effect of selected design-of-experiment parameters.

Cutting Fluid	Speed (RPM)	Depth of Cut (mm)	Feed (mm/rev)	Flank Wear (mm)			Average of Wear (mm)
Dry	605	0.3	0.031	0.1395	0.1311	0.1353	0.1353
Dry	1330	0.4	0.034	0.2366	0.241	0.2326	0.2367
Dry	2000	0.5	0.038	0.7525	0.7526	0.7611	0.7554
SO	605	0.3	0.034	0.0844	0.0931	0.0930	0.0901
SO	1330	0.4	0.038	0.1353	0.1330	0.1353	0.1345
SO	2000	0.5	0.031	0.3573	0.3531	0.3488	0.3530
CO	605	0.4	0.031	0.1205	0.1120	0.1078	0.1134
CO	1330	0.5	0.034	0.1668	0.1586	0.1628	0.1627
CO	2000	0.3	0.038	0.1966	0.1966	0.1860	0.1930
CO1	605	0.5	0.038	0.0972	0.0972	0.0972	0.0972
CO1	1330	0.3	0.031	0.1586	0.1543	0.1586	0.1571
CO1	2000	0.4	0.034	0.5475	0.5475	0.5476	0.5475
CO2	605	0.4	0.038	0.1078	0.1078	0.0972	0.1042
CO2	1330	0.5	0.031	0.1015	0.0888	0.1078	0.0993
CO2	2000	0.3	0.034	0.2833	0.2832	0.2874	0.2846
CO3	605	0.5	0.034	0.1669	0.1170	0.1274	0.1371
CO3	1330	0.3	0.038	0.0655	0.0761	0.0655	0.0690
CO3	2000	0.4	0.031	0.7130	0.7188	0.7188	0.7168

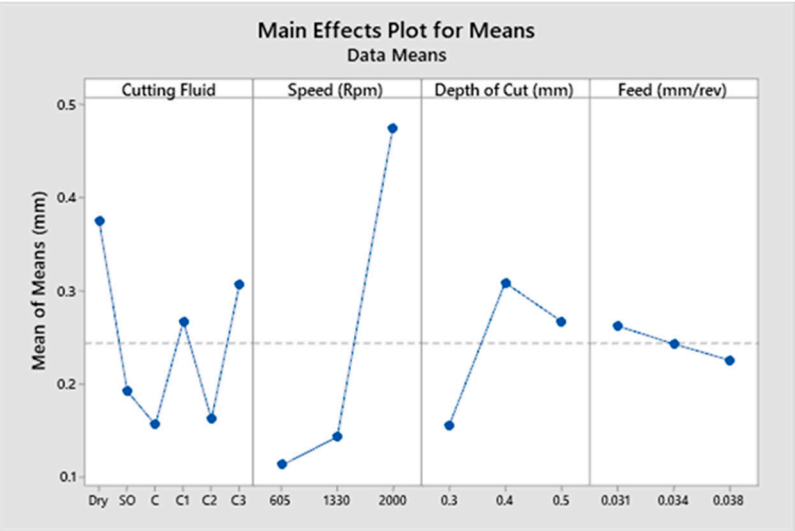


Figure 12. Main effects plot for means of flank tool wear value (mm).

The application of SO lubrication reduced the mean flank wear by 48.7% compared to dry machining, with a mean value of 0.19 mm. While this cutting fluid effectively reduced cutting zone temperatures and minimized thermal softening, its boundary lubrication performance remained limited due to the short-chain hydrocarbon structure of mineral oils. In the case of SO lubricant, two primary mechanisms were found to operate synergistically. First, the absence of effective cooling led to thermal cracking from cyclic thermal stresses, creating micro-fractures in the insert material as shown in Figure 13c. Secondly, adhesive wear took place as a consequence, leading to some BUE according to the EDX results shown in Figure 13c. These findings align with established research on the machining of hardened steels [78,79]. The limitations of SO lubrication became apparent when comparing SO's performance to cactus oil blends, particularly at higher cutting speeds where the mineral oil's lubricating film broke down more readily. The results corroborate previous studies on conventional cutting fluids in steel machining applications [5,6,9].

CO demonstrated better performance than soluble oil and dry conditions, reducing the mean flank wear (0.156 mm) by 19% and 58%, respectively. The vegetable oil's effectiveness stems from its unique fatty acid composition. These long-chain unsaturated fatty acids form durable chemisorbed films on metal surfaces through their polar carboxyl groups, creating an effective boundary lubrication layer. Furthermore, the natural antioxidants present in cactus oil, such as tocopherols, provided enhanced oxidative stability at elevated temperatures, preventing the rapid lubricant breakdown observed with mineral-based soluble fluid [20]. This combination of properties resulted in reduced tool wear, as shown in Figure 13d.

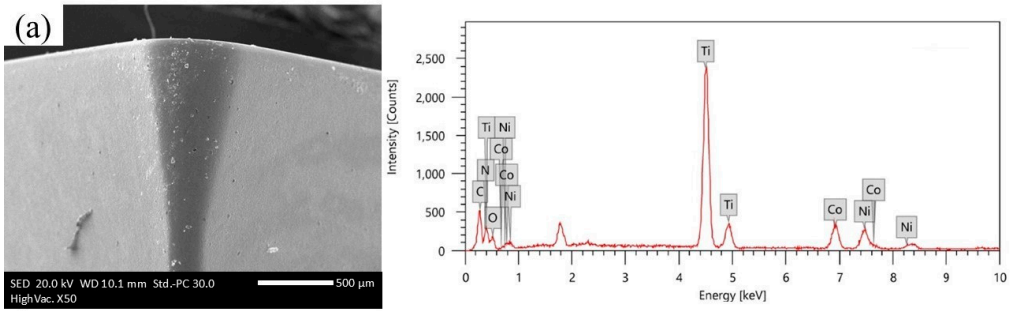


Figure 13. *Cont.*

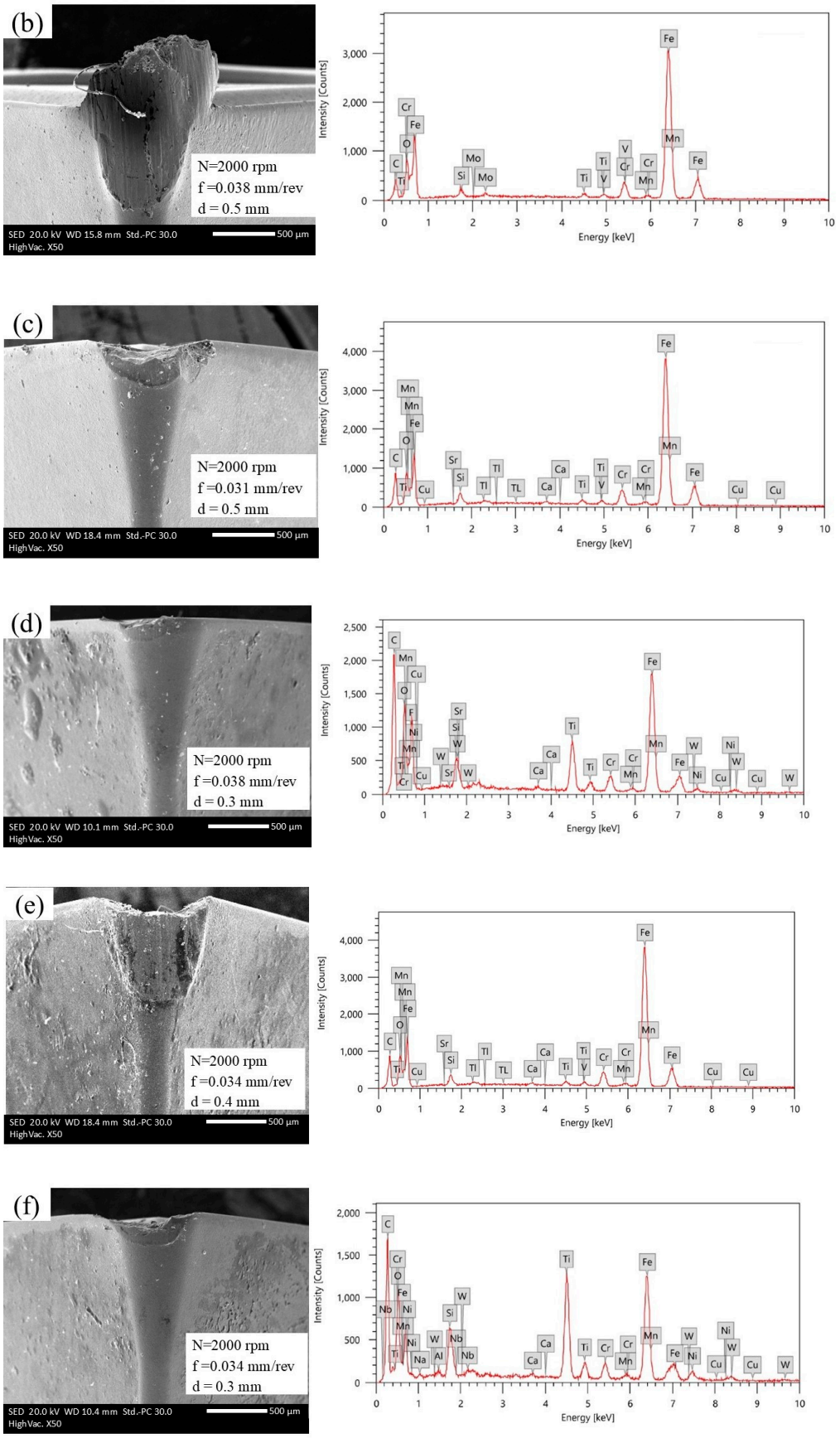


Figure 13. *Cont*.

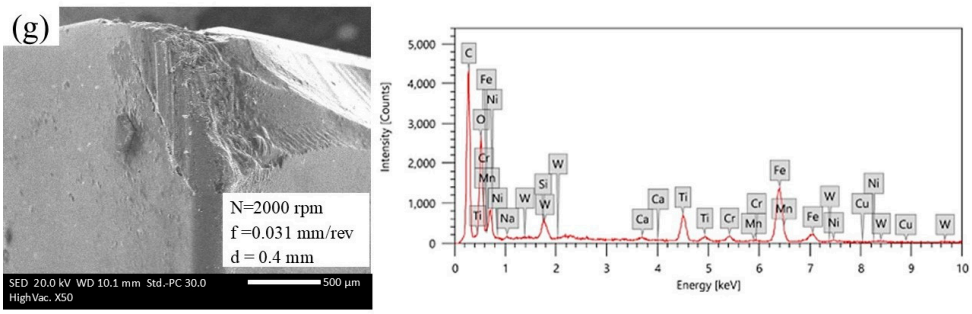


Figure 13. SEM and EDX images of the cutting inserts under various cutting conditions and lubrication methods: (**a**) insert prior to cutting, (**b**) dry conditions, (**c**) SO lubricant, (**d**) CO lubricant, (**e**) CO1 lubricant, (**f**) CO2 lubricant, and (**g**) CO3 lubricant.

The formulations of nano-enhanced cactus oil with low concentrations of ACNPs demonstrated comparable advancements in tool protection with respect to CO samples. CO1 (0.025 wt.% ACNPs) illustrated a decrease in abrasive tool wear, as depicted in Figure 13e. However, the EDX analysis reveals clear evidence of workpiece material transfer, indicated by the presence of the Fe element concentration at the tool flank.

The CO2 (0.05 wt.% ACNP) blend achieved the best overall performance (0.16 mm mean flank wear), as shown in Figure 13f. The activated carbon nanoparticles functioned through multiple mechanisms to enhance lubrication. Their microporous structure with a large surface area acted as a reservoir for cutting oil, ensuring continuous lubricant replenishment at the tool–workpiece interface. Simultaneously, the nanoparticles filled the surface asperities, reducing direct metal contact and minimizing abrasive wear. The polar functional groups on the ACNP surfaces, including hydroxyl and carboxyl moieties, enhanced adhesion to both the tool and workpiece surfaces, creating a more robust tribofilm.

Nonetheless, increasing the carbon concentration to 0.1 wt.% in (CO3 samples) led to considerable tool breakage, heightened abrasive wear, and substantial loss of tool material, as presented in Figure 13g. This is also evidenced by the decreased titanium concentration in the EDX analysis results. One possible reason behind this deterioration in performance is the potential particle agglomeration of ACNPs at this stage of work, which not only diminished the efficacy of the cutting fluid but also generated a mechanism for abrasive wear at the tool flank surface.

Cutting parameters significantly influenced flank wear development across all lubrication conditions. Increasing the cutting speed from 605 to 2000 rpm worsened the flank wear by five times (Figure 12) due to elevated temperatures and thermal softening effects. The depth of cuts showed a fluctuating trend, with the tool wear increasing by 99% from 0.3 mm to 0.4 mm cuts as tool engagement forces grew substantially. Interestingly, a slight decrease in tool wear (13%) was observed when increasing the depth of cuts from 0.4 mm to 0.5 mm. Interactions with other parameters might have played a role in this alternating behavior. The feed rate exhibited a more linear relationship, with high feeds (0.038 mm/rev) producing better results of tool wear.

The research work in [49] exploited hybrid nano-additives with ionic liquid, ZnO, and graphene in rapeseed oil. The wettability of plain rapeseed oil was found to be 24°, while rapeseed with hybrid nano-additives reached 10°. In the current research work, cactus oil achieved a contact angle of 25.8°, and CO2 enhanced this value to 15.5°. Both rapeseed oil and cactus oil showed Newtonian behavior at nearly all shear rates. The addition of nano-additives to rapeseed oil increased the dynamic viscosity in the range of 2% to 180%. Similar behavior was observed in the current findings, where the addition of ACNPs increased the dynamic viscosity by 9–15% at 40°.

Mushtaq et al. [51] found that adding 0.5% graphene to jatropha oil significantly reduced the coefficient of friction (COF) by 44% and wear by 43.7% compared to the base oil. The outcomes are found to be similar to the results of this work, in which blending ACNPs with cactus oil at low concentrations reduced the coefficient of friction by 32% and tool wear by 57% compared to dry conditions. In another work, Ruitao Peng et al. [80] also reported that the addition of graphene nanoparticles to palm oil reduced the coefficient of friction by 6.80–17.04% and surface roughness by 7.35–20.33%, while adding activated carbon nanoparticles to cactus oil in this study enhanced surface roughness by 35% compared to dry conditions.

3.7. Cost Analysis

Lubricants are essential in machining processes, as they not only improve performance but also have a significant impact on operational costs. The choice and pricing of lubricants directly affect the economic viability of the machining operation, influencing factors such as tool life, surface quality, and overall productivity. High-quality lubricants minimize wear on cutting tools, which extends tool life and reduces the frequency of replacements, ultimately leading to substantial cost savings over time [81].

Given the increasing focus on sustainability and cost efficiency, selecting the right lubricant is critical in contemporary manufacturing. Table 8 compares the cost-effectiveness of cactus oil blends with commercial mineral-based cutting fluids, highlighting factors such as material and preparation costs, tool life impact, and environmental considerations. The cost of cactus oil in local Egyptian markets ranges between USD 8 and USD 10 per liter, while the price of activated carbon varies from USD 10 to USD 15 per gram. In contrast, commercial cutting fluids such as soluble oil are priced at USD 4 per liter. The overall expense associated with employing MQL alongside cactus oil (100 mL) and 0.05 wt.% activated carbon for a turning operation on H13 steel is roughly USD 1.53. Additionally, the expenditure for utilizing 100 mL of soluble oil, which is priced at USD 4 per liter, amounts to USD 0.40.

Table 8. Cost comparison between cactus oil blends and commercial mineral-based cutting fluids.

Cost Factor	Cactus Oil + ACNPs	Commercial Cutting Fluids
Material Cost	Higher (due to nanoparticle infusion and extraction)	Lower (bulk availability)
Preparation Cost	Moderate (requires filtration, nanoparticle mixing)	Low (ready-to-use)
Tool Life Impact	Potentially longer (better lubrication reduces wear)	Moderate (depends on additives)
Machining Efficiency	Comparable or better (lower friction, heat dissipation)	Standard performance
Disposal and Environmental Cost	Low (biodegradable, non-toxic)	High (hazardous waste treatment)
Health and Safety Costs	Low (non-toxic, no skin irritation)	High (exposure risks, PPE required)
Maintenance and System Longevity	Better (less residue, cleaner machines)	Higher (sludge buildup, corrosion)

Table 9 provides a detailed breakdown of the cost of cactus oil infused with ACNPs versus commercial cutting fluids, emphasizing the relatively higher base material costs of cactus oil due to extraction and nanoparticle infusion. Despite these higher upfront costs, cactus oil offers advantages in terms of tool life and environmental sustainability. Furthermore, a study by Talib et al. [42] demonstrated that a nanofluid blend (MJO + 0.025 wt.% AC) delivered a 17% increase in tool life compared to standard cutting fluids during turning operations. Since the study outcomes showed similar results of tool

wear to the current work, this enhancement in the tool life is adopted in the cost calculations and comparison between the cactus oil and soluble oil. The tool life improvement translates into significant cost savings when comparing the tool wear rates and replacement costs between cactus oil blends (e.g., CO2) and commercial fluids. Using bio-oil with nano-additives could save machining shops USD 50–100 monthly in tool replacement costs if they use 10 tools per month at USD 10 per tool. This evidence underscores the importance of choosing the right lubricant blend for machining applications, balancing cost, efficiency, and sustainability.

Table 9. Detailed cost analysis of cactus oil with activated carbon nanoparticles (ACNPs) vs. commercial cutting fluids in machining operations.

Component	Cactus Oil + ACNPs	Commercial Synthetic Cutting Fluid
Base Fluid Cost	USD 8–10/L (extraction and refining)	USD 4/L (petroleum-based)
Nanoparticle Additives	USD 10–15/g (activated carbon)	USD 0 (pre-mixed additives)
Tool Replacement Cost	USD 50–100 saved per tool	Standard wear
Tool Wear Rate	20–30% lower (due to superior lubrication)	Baseline

4. Conclusions and Future Work

This study presents a novel, sustainable approach to metal cutting operations by developing nano-MQL cactus oil as an eco-friendly alternative to conventional mineral-based cutting fluids. The key innovation lies in the integration of activated carbon nanoparticles (ACNPs) derived from recycled plastic waste, which significantly enhances the physico-chemical, rheological, and tribological properties of cactus oil. The findings from testing cactus oil blends, particularly those containing 0.05 wt.% ACNPs, present a viable solution that addresses current critical challenges in sustainable manufacturing, such as toxicity, non-biodegradability, and poor lubrication performance associated with traditional cutting fluids. The key findings are listed as follows:

- Plain cactus oil exhibited a 34% improvement in wettability compared to commercial soluble oil, with further enhancements of up to 60% when blended with 0.05 wt.% ACNPs. This suggests adequate fluid penetration into the tool–workpiece interface, reducing friction and heat generation.
- Cactus oil demonstrated Newtonian behavior with a high viscosity index (283.21), outperforming commercial soluble oil. The addition of ACNPs increased the dynamic viscosity of cactus oil by 9–15% at 40 °C. This enhancement demonstrates superior thermal stability and shear resistance compared to plain cactus oil. This viscosity enhancement is critical for maintaining effective lubrication under varying machining conditions. It also promotes the formation of an adequate oil film thickness without compromising fluid flow characteristics, especially during MQL system application.
- Tribological evaluation revealed that nano-enhanced cactus oil formulations substantially outperformed plain cactus oil in boundary lubrication regimes, where metal-to-metal contact is most prevalent during machining operations. The coefficient of friction of the mixtures was reduced by up to 32%, as compared to the plain cactus sample.
- These significant reductions in friction explain the observed 15.5% and 23.6% reductions in tool flank wear and surface roughness in the case of applying cactus oil with 0.05 wt.% ACNP blend, compared to soluble oil. The mechanism can be attributed to the nanoscale ACNP particles effectively filling surface asperities and creating a

more stable tribofilm at the tool–workpiece interface, which was further evidenced by post-machining surface analysis showing more uniform wear patterns compared to conventional cutting fluids.

- The integration of recycled nano-additives and non-food-based vegetable oil not only enhances cutting performance but also offers a cost-effective and environmentally responsible solution. This dual benefit positions cactus oil-based nanofluids as promising candidates for widespread adoption in sustainable metalworking operations.

The use of non-edible cactus oil and ACNPs from recycled plastic waste aligns with circular economy principles, offering a biodegradable, non-toxic solution that avoids competition with food resources and reduces industrial waste. To further advance this research, future studies are recommended to study the long-term dispersion stability of ACNPs in cactus oil under varying storage and operational conditions to ensure practical applicability. Also, a future study is planned to evaluate the synergistic effects of hybrid nano-additives (ACNPs with graphene or MoS_2) to further enhance thermal conductivity, load-carrying capacity, and anti-wear properties. Another consideration for future work is conducting large-scale industrial trials to validate the practical applicability and economic feasibility of the proposed nanofluid on other metal cutting processes.

Author Contributions: Conceptualization, G.A.N., I.M., F.P. and M.A.D.; methodology, M.G.A.N., B.G.N. and I.M.; sample preparation, N.K.E., B.G.N. and M.G.A.N.; validation, M.G.A.N., B.G.N. and N.K.E.; formal analysis, N.K.E., M.G.A.N., B.G.N. and I.M.; investigation, M.G.A.N., N.K.E. and B.G.N.; resources, G.A.N. and F.P.; data curation, F.P., B.G.N. and I.M.; writing—original draft preparation, N.K.E., F.P. and M.G.A.N.; writing—review and editing, G.A.N., M.A.D. and I.M.; visualization, N.K.E. and B.G.N.; project administration, G.A.N. All authors have read and agreed to the published version of the manuscript.

Funding: This research received no external funding.

Data Availability Statement: Correspondence and requests for materials should be addressed to N.K.E. All the data in this study are included in the submitted manuscript. For further data, please contact the corresponding author (N.K.E.) via nada.elbadway@ejust.edu.eg or eng-nada.kamel1621@alexu.edu.eg.

Conflicts of Interest: The authors declare that they have no conflicts of interest.

References

1. Malek, J.; Desai, T.N. A Framework for Prioritizing the Solutions to Overcome Sustainable Manufacturing Barriers. *Clean. Logist. Supply Chain* **2021**, *1*, 100004. [CrossRef]
2. Maruthi, G.D.; Rashmi, R. Green Manufacturing: It's Tools and Techniques That Can Be Implemented in Manufacturing Sectors. *Mater. Today Proc.* **2015**, *2*, 3350–3355. [CrossRef]
3. Yuan, Y. *A System Approach for Reducing the Environmental Impact of Manufacturing and Sustainability Improvement of Nano-Scale Manufacturing*; University of California: Berkeley, CA, USA, 2005.
4. Sarhan, A.A.D.; Matsubara, A. Compensation Method of the Machine Tool Spindle Thermal Displacement for Accurate Monitoring of Cutting Forces. *Mater. Manuf. Process.* **2011**, *26*, 1511–1521. [CrossRef]
5. Hamdan, A.; Sarhan, A.A.D.; Hamdi, M. An Optimization Method of the Machining Parameters in High-Speed Machining of Stainless Steel Using Coated Carbide Tool for Best Surface Finish. *Int. J. Adv. Manuf. Technol.* **2012**, *58*, 81–91. [CrossRef]
6. Adler, D.P.; Hii, W.W.-S.; Michalek, D.J.; Sutherland, J.W. Examining the Role of Cutting Fluids in Machining and Efforts to Address Associated Environmental/Health Concerns. *Mach. Sci. Technol.* **2006**, *10*, 23–58. [CrossRef]
7. Pape, F.; Poll, G.; Ellersiek, L.; Denkena, B.; Liu, H. Tribological Effects of Metalworking Fluids in Cutting Processes. *Lubricants* **2023**, *11*, 224. [CrossRef]
8. Liu, H.C.; Pape, F.; Zhao, Y.; Ellersiek, L.; Denkena, B.; Poll, G. On the Elastohydrodynamic Film-Forming Properties of Metalworking Fluids and Oil-in-Water Emulsions. *Tribol. Lett.* **2022**, *71*, 10. [CrossRef]
9. Talib, N.; Rahim, E.A. Performance of Modified Jatropha Oil in Combination with Hexagonal Boron Nitride Particles as a Bio-Based Lubricant for Green Machining. *Tribol. Int.* **2018**, *118*, 89–104. [CrossRef]

10. Wang, X.; Huang, J.; Guo, Z. Overview of the Development of Slippery Surfaces: Lubricants from Presence to Absence. *Adv. Colloid Interface Sci.* **2022**, *301*, 102602. [CrossRef]
11. Pape, F.; Nassef, B.G.; Schmölzer, S.; Stobitzer, D.; Taubmann, R.; Rummel, F.; Stegmann, J.; Gerke, M.; Marian, M.; Poll, G.; et al. Comprehensive Evaluation of the Rheological, Tribological, and Thermal Behavior of Cutting Oil and Water-Based Metalworking Fluids. *Lubricants* **2025**, *13*, 219. [CrossRef]
12. Huang, J.-W.; Bai, Y.-Y.; Zeeshan, M.; Liu, R.-Q.; Dong, G.-H. Effects of Exposure to Chlorinated Paraffins on Human Health: A Scoping Review. *Sci. Total Environ.* **2023**, *886*, 163953. [CrossRef] [PubMed]
13. Shashidhara, Y.M.; Jayaram, S.R. Vegetable Oils as a Potential Cutting Fluid—An Evolution. *Tribol. Int.* **2010**, *43*, 1073–1081. [CrossRef]
14. Koller, M.F.; Foulds, I.S. Cutting Fluids. In *Kanerva's Occupational Dermatology*; John, S.M., Johansen, J.D., Rustemeyer, T., Elsner, P., Maibach, H.I., Eds.; Springer International Publishing: Cham, Switzerland, 2019; pp. 1–19. ISBN 978-3-319-40221-5.
15. Bennett, E.O.; Bennett, D.L. Minimizing Human Exposure to Chemicals in Metalworking Fluids. *Lubr. Eng.* **1987**, *43*, 167–175.
16. Woma, T.Y.; Lawal, S.A.; Abdulrahman, A.S.; Olutoye, M.A.; Ojapah, M.M. Vegetable Oil Based Lubricants: Challenges and Prospects. *Tribol. Online* **2019**, *14*, 60–70. [CrossRef]
17. Tavella, R.A.; da Silva Júnior, F.M.R.; Santos, M.A.; Miraglia, S.G.E.K.; Pereira Filho, R.D. A Review of Air Pollution from Petroleum Refining and Petrochemical Industrial Complexes: Sources, Key Pollutants, Health Impacts, and Challenges. *ChemEngineering* **2025**, *9*, 13. [CrossRef]
18. Sankaranarayanan, R.; Krolczyk, G.M. A Comprehensive Review on Research Developments of Vegetable-Oil Based Cutting Fluids for Sustainable Machining Challenges. *J. Manuf. Process.* **2021**, *67*, 286–313. [CrossRef]
19. Wu, X.; Li, C.; Zhou, Z.; Nie, X.; Chen, Y.; Zhang, Y.; Cao, H.; Liu, B.; Zhang, N.; Said, Z.; et al. Circulating Purification of Cutting Fluid: An Overview. *Int. J. Adv. Manuf. Technol.* **2021**, *117*, 2565–2600. [CrossRef]
20. Fox, N.J.; Stachowiak, G.W. Vegetable Oil-Based Lubricants—A Review of Oxidation. *Tribol. Int.* **2007**, *40*, 1035–1046. [CrossRef]
21. Kuram, E.; Ozcelik, B.; Demirbas, E. Environmentally Friendly Machining: Vegetable Based Cutting Fluids. In *Green Manufacturing Processes and Systems*; Davim, J.P., Ed.; Springer: Berlin/Heidelberg, Germany, 2013; pp. 23–47. ISBN 978-3-642-33792-5.
22. Pranav, P.; Sneha, E.; Rani, S. Vegetable Oil-Based Cutting Fluids and Its Behavioral Characteristics in Machining Processes: A Review. *Ind. Lubr. Tribol.* **2021**, *73*, 1159–1175. [CrossRef]
23. Bork, C.A.S.; de Gonçalves, J.F.S.; de Gomes, J.O.; Gheller, J. Performance of the Jatropha Vegetable-Base Soluble Cutting Oil as a Renewable Source in the Aluminum Alloy 7050-T7451 Milling. *CIRP J. Manuf. Sci. Technol.* **2014**, *7*, 210–221. [CrossRef]
24. Villarrazo, N.; Caneda, S.; Pereira, O.; Rodríguez, A.; López de Lacalle, L.N. The Effects of Lubricooling Ecosustainable Techniques on Tool Wear in Carbon Steel Milling. *Materials* **2023**, *16*, 2936. [CrossRef] [PubMed]
25. Subramaniam, S.; Thangamuthu, M. Influence of Vegetable Based Cutting Fluids on Cutting Force and Vibration Signature during Milling of Aluminium Metal Matrix Composites. *J. Tribol.* **2017**, *12*, 1–17.
26. Pereira, O.; Martín-Alfonso, J.E.; Rodríguez, A.; Calleja, A.; Fernández-Valdivielso, A.; López de Lacalle, L.N. Sustainability Analysis of Lubricant Oils for Minimum Quantity Lubrication Based on Their Tribo-Rheological Performance. *J. Clean. Prod.* **2017**, *164*, 1419–1429. [CrossRef]
27. Winter, M.; Öhlschläger, G.; Dettmer, T.; Ibbotson, S.; Kara, S.; Herrmann, C. Using Jatropha Oil Based Metalworking Fluids in Machining Processes: A Functional and Ecological Life Cycle Evaluation. In *Leveraging Technology for a Sustainable World, Proceedings of the 19th CIRP Conference on Life Cycle Engineering, University of California at Berkeley, Berkeley, USA, 23–25 May 2012*; Dornfeld, D.A., Linke, B.S., Eds.; Springer: Berlin/Heidelberg, Germany, 2012; pp. 311–316.
28. Pereira, O.; Català, P.; Rodríguez, A.; Ostra, T.; Vivancos, J.; Rivero, A.; López-De-Lacalle, L.N. The Use of Hybrid CO2+MQL in Machining Operations. *Procedia Eng.* **2015**, *132*, 492–499. [CrossRef]
29. Pereira, O.; Urbikain, G.; Rodríguez, A.; Fernández-Valdivielso, A.; Calleja, A.; Ayesta, I.; de Lacalle, L.N.L. Internal Cryolubrication Approach for Inconel 718 Milling. *Procedia Manuf.* **2017**, *13*, 89–93. [CrossRef]
30. López De Lacalle, L.N.; Angulo, C.; Lamikiz, A.; Sánchez, J.A. Experimental and Numerical Investigation of the Effect of Spray Cutting Fluids in High Speed Milling. *J. Mater. Process. Technol.* **2006**, *172*, 11–15. [CrossRef]
31. Farfan-Cabrera, L.I.; Aguilar-Rosas, O.A.; Pérez-González, J.; Marín-Santibañez, B.M.; Rodríguez-González, F. Viscoelastic Water-Based Lubricants with Nopal Cactus Mucilage as Green Metalworking Fluids. *Lubricants* **2024**, *12*, 56. [CrossRef]
32. Elbadawy, N.K.; Daha, M.A.; Nassef, G.A.; Maher, I. Investigating the Feasibility of Utilising Cactus Oil as a Minimum Quantity Lubrication Eco-Friendly Coolant for Machining 42CrMo4 Stee. *Int. J. Mach. Mach. Mater.* **2025**, 1–27. [CrossRef]
33. Nounah, I.; El Harkaoui, S.; Hajib, A.; Gharby, S.; Harhar, H.; Bouyahya, A.; Caprioli, G.; Maggi, F.; Matthäus, B.; Charrouf, Z. Effect of Seed's Geographical Origin on Cactus Oil Physico-Chemical Characteristics, Oxidative Stability, and Antioxidant Activity. *Food Chem. X* **2024**, *22*, 101445. [CrossRef]
34. Al-Naqeb, G.; Fiori, L.; Ciolli, M.; Aprea, E. Prickly Pear Seed Oil Extraction, Chemical Characterization and Potential Health Benefits. *Molecules* **2021**, *26*, 5018. [CrossRef]

35. Loizzo, M.R.; Bruno, M.; Balzano, M.; Giardinieri, A.; Pacetti, D.; Frega, N.G.; Sicari, V.; Leporini, M.; Tundis, R. Comparative Chemical Composition and Bioactivity of Opuntia Ficus-Indica Sanguigna and Surfarina Seed Oils Obtained by Traditional and Ultrasound-Assisted Extraction Procedures. *Eur. J. Lipid Sci. Technol.* **2019**, *121*, 1800283. [CrossRef]
36. Berraaouan, A.; Ziyyat, A.; Mekhfi, H.; Marianne, S.; Fauconnier, M.-L.; Abdelkhaleq, L.; Mohammed, A.; Bnouham, M. Chemical Composition of Cactus Pear Seed Oil: Phenolics Identification and Antioxidant Activity. *J. Pharmacopunct.* **2022**, *25*, 121–129. [CrossRef]
37. El Mannoubi, I.; Barrek, S.; Skanji, T.; Casabianca, H.; Zarrouk, H. Characterization of Opuntia Ficus Indica Seed Oil from Tunisia. *Chem. Nat. Compd.* **2009**, *45*, 616–620. [CrossRef]
38. Chougui, N.; Tamendjari, A.; Hamidj, W.; Hallal, S.; Barras, A.; Richard, T.; Larbat, R. Oil Composition and Characterisation of Phenolic Compounds of Opuntia Ficus-Indica Seeds. *Food Chem.* **2013**, *139*, 796–803. [CrossRef]
39. Sancheti, S.V.; Yadav, G.D. Synthesis of Environment-Friendly, Sustainable, and Nontoxic Bio-Lubricants: A Critical Review of Advances and a Path Forward. *Biofuels Bioprod. Biorefining* **2022**, *16*, 1172–1195. [CrossRef]
40. Berman, D. Plant-Based Oils for Sustainable Lubrication Solutions—Review. *Lubricants* **2024**, *12*, 300. [CrossRef]
41. Bhaumik, S.; Maggirwar, R.; Datta, S.; Pathak, S.D. Analyses of Anti-Wear and Extreme Pressure Properties of Castor Oil with Zinc Oxide Nano Friction Modifiers. *Appl. Surf. Sci.* **2018**, *449*, 277–286. [CrossRef]
42. Talib, N.; Sabri, A.M.; Zolkefli, A.A.; Tan, K.S.; Kunar, S.; Mekanikal, F.K.; Pembuatan, D. Tribological Enhancement of Modified Jatropha Oil by Activated Carbon Nanoparticle for Metalworking Fluid Application. *J. Tribol.* **2022**, *33*, 113–124.
43. Seid Ahmed, Y.; Hernández González, L. Ti6Al4V Grinding Using Different Lubrication Modes for Minimizing Energy Consumption. *Int. J. Adv. Manuf. Technol.* **2023**, *126*, 2387–2405. [CrossRef]
44. Gaurav, G.; Sharma, A.; Dangayach, G.S.; Meena, M.L. Assessment of Jojoba as a Pure and Nano-Fluid Base Oil in Minimum Quantity Lubrication (MQL) Hard-Turning of Ti–6Al–4V: A Step towards Sustainable Machining. *J. Clean. Prod.* **2020**, *272*, 122553. [CrossRef]
45. Liu, W.; Qiao, X.; Liu, S.; Chen, P. A Review of Nanomaterials with Different Dimensions as Lubricant Additives. *Nanomaterials* **2022**, *12*, 3780. [CrossRef] [PubMed]
46. Duan, L.; Li, J.; Duan, H. Nanomaterials for Lubricating Oil Application: A Review. *Friction* **2023**, *11*, 647–684. [CrossRef]
47. Syahir, A.Z.; Zulkifli, N.W.M.; Masjuki, H.H.; Kalam, M.A.; Alabdulkarem, A.; Gulzar, M.; Khuong, L.S.; Harith, M.H. A Review on Bio-Based Lubricants and Their Applications. *J. Clean. Prod.* **2017**, *168*, 997–1016. [CrossRef]
48. Bai, X.; Li, C.; Dong, L.; Yin, Q. Experimental Evaluation of the Lubrication Performances of Different Nanofluids for Minimum Quantity Lubrication (MQL) in Milling Ti-6Al-4V. *Int. J. Adv. Manuf. Technol.* **2019**, *101*, 2621–2632. [CrossRef]
49. Nassef, B.G.; Pape, F.; Poll, G. Enhancing the Performance of Rapeseed Oil Lubricant for Machinery Component Applications through Hybrid Blends of Nanoadditives. *Lubricants* **2023**, *11*, 479. [CrossRef]
50. Talib, N.; Sani, A.S.A.; Hamzah, N. Modified Jatropha Nano-Lubricant as Metalworking Fluid for Machining Process. *J. Tribol.* **2019**, *23*, 90–96.
51. Mushtaq, Z. Enhancing the Tribological Characteristics of Jatropha Oil Using Graphene Nanoflakes. *J. Tribol.* **2021**, *28*, 129–143.
52. Sharma, V.S.; GurRaj, S.; Sørby, K. A Review on Minimum Quantity Lubrication for Machining Processes. *Mater. Manuf. Process.* **2015**, *30*, 935–953. [CrossRef]
53. Li, C.H.; Li, J.Y.; Wang, S.; Zhang, Q. Modeling and Numerical Simulation of the Grinding Temperature Field with Nanoparticle Jet of MQL. *Adv. Mech. Eng.* **2013**, *5*, 986984. [CrossRef]
54. Shahrom, M.S.; Yahya, N.M.; Yusoff, A.R. Taguchi Method Approach on Effect of Lubrication Condition on Surface Roughness in Milling Operation. *Procedia Eng.* **2013**, *53*, 594–599. [CrossRef]
55. Patole, P.B.; Kulkarni, V.V.; Bhatwadekar, S.G. MQL Machining with Nano Fluid: A Review. *Manuf. Rev.* **2021**, *8*, 13. [CrossRef]
56. Rifat, M.; Rahman, M.H.; Das, D. A Review on Application of Nanofluid MQL in Machining. In Proceedings of the AIP Conference Proceedings, Provo, UT, USA, 16–21 July 2017; American Institute of Physics Inc.: College Park, MD, USA, 2017; Volume 1919, pp. 1–10.
57. Bai, X.; Zhou, F.; Li, C.; Dong, L.; Lv, X.; Yin, Q. Physicochemical Properties of Degradable Vegetable-Based Oils on Minimum Quantity Lubrication Milling. *Int. J. Adv. Manuf. Technol.* **2020**, *106*, 4143–4155. [CrossRef]
58. Thakur, A.; Manna, A.; Samir, S. Experimental Investigation of Nanofluids in Minimum Quantity Lubrication during Turning of EN-24 Steel. *Proc. Inst. Mech. Eng. Part J J. Eng. Tribol.* **2019**, *234*, 712–729. [CrossRef]
59. Sahoo, S.P.; Datta, S. Dry, MQL, and Nanofluid MQL Machining of Ti–6Al–4V Using Uncoated WC–Co Insert: Application of Jatropha Oil as Base Cutting Fluid and Graphene Nanoplatelets as Additives. *Arab. J. Sci. Eng.* **2020**, *45*, 9599–9618. [CrossRef]
60. Nassef, M.G.A.; Hassan, H.S.; Nassef, G.A.; Nassef, B.G.; Soliman, M.; Elkady, M.F. Activated Carbon Nano-Particles from Recycled Polymers Waste as a Novel Nano-Additive to Grease Lubrication. *Lubricants* **2022**, *10*, 214. [CrossRef]
61. Pereira, L.; Castillo, V.; Calero, M.; Blázquez, G.; Solís, R.R.; Martín-Lara, M.Á. Insights into Using Plastic Waste to Produce Activated Carbons for Wastewater Treatment Applications: A Review. *J. Water Process. Eng.* **2024**, *62*, 105386. [CrossRef]

62. *ASTM D92-23*; Standard Test Method for Flash and Fire Points by Cleveland Open Cup Tester. ASTM International: West Conshohocken, PA, USA, 2023.
63. *ASTM D2196-20*; Standard Test Methods for Rheological Properties of Non-Newtonian Materials by Rotational (Brookfield Type) Viscometer. ASTM International: West Conshohocken, PA, USA, 2020.
64. *ASTM D4172-23*; Standard Test Method for Wear Preventive Characteristics of Lubricating Fluid (Four-Ball Method). ASTM International: West Conshohocken, PA, USA, 2023.
65. *ISO 4287:1997*; Geometrical Product Specifications (GPS)—Surface texture: Profile method—Terms, definitions and surface texture parameters. International Organization for Standardization: Geneva, Switzerland, 1997.
66. *ISO 3685:1993*; Tool-life testing with single-point turning tools. International Organization for Standardization: Geneva, Switzerland, 1993.
67. El Bouazzaoui, Y.; Habsaoui, A.; Ouaddari, H.; Touhami, M.E. Geographic Impact on Opuntia Ficus-Indica Seeds: Oil and Phenolic Compound Extraction and Characterization. *S. Afr. J. Bot.* **2023**, *159*, 605–616. [CrossRef]
68. Taoufik, F.; Zine, S.; El Hadek, M.; Hassani, L.I.; Gharby, S.; Harhar, H.; Matthäus, B. Oil Content and Main Constituents of Cactus Seed Oils Opuntia Ficus Indica of Different Origin in Morocco. *Mediterr. J. Nutr. Metab.* **2015**, *8*, 85–92. [CrossRef]
69. Sawaya, W.N.; Khan, P. Chemical Characterization of Prickly Pear Seed Oil, Opuntia Ficus-Indica. *J. Food Sci.* **1982**, *47*, 2060–2061. [CrossRef]
70. Lundgren, S.M.; Ruths, M.; Danerlöv, K.; Persson, K. Effects of Unsaturation on Film Structure and Friction of Fatty Acids in a Model Base Oil. *J. Colloid Interface Sci.* **2008**, *326*, 530–536. [CrossRef]
71. Tahoon, M.A.; Siddeeg, S.M.; Alsaiari, N.S.; Mnif, W.; Ben Rebah, F. Effective Heavy Metals Removal Fromwater Using Nanomaterials: A Review. *Processes* **2020**, *8*, 645. [CrossRef]
72. Yang, X.; Wan, Y.; Zheng, Y.; He, F.; Yu, Z.; Huang, J.; Wang, H.; Ok, Y.S.; Jiang, Y.; Gao, B. Surface Functional Groups of Carbon-Based Adsorbents and Their Roles in the Removal of Heavy Metals from Aqueous Solutions: A Critical Review. *Chem. Eng. J.* **2019**, *366*, 608–621. [CrossRef] [PubMed]
73. López-Barrón, C.R.; Wagner, N.J.; Porcar, L. Layering, Melting, and Recrystallization of a Close-Packed Micellar Crystal under Steady and Large-Amplitude Oscillatory Shear Flows. *J. Rheol.* **2015**, *59*, 793–820. [CrossRef]
74. Yan, Y.D.; Dhont, J.K.G.; Smits, C.; Lekkerkerker, H.N.W. Oscillatory-Shear-Induced Order in Nonaqueous Dispersions of Charged Colloidal Spheres. *Phys. A Stat. Mech. Its Appl.* **1994**, *202*, 68–80. [CrossRef]
75. Bao, J.; Heyd, R.; Régnier, G.; Ammar, A.; Peixinho, J. Viscosity of Graphene in Lubricating Oil, Ethylene Glycol and Glycerol. *Res. Sq.* **2023**, *148*, 11455–11465. [CrossRef]
76. Hassan, M.; Samion, S.; Ani, F. The Tribological Characteristics of the Cactus and Mineral Oil Blends Using Four-Ball Tribotester. *J. Teknol.* **2016**, *78*, 33–38. [CrossRef]
77. Holmberg, K.; Erdemir, A. Influence of Tribology on Global Energy Consumption, Costs and Emissions. *Friction* **2017**, *5*, 263–284. [CrossRef]
78. Stachowiak, G.; Andrew, W.B. *Engineering Tribology*, 4th ed.; Elsevier: Amsterdam, The Netherlands, 2013.
79. Neog, S.P.; Kumar, A.R.; Bakshi, S.D.; Das, S. Understanding the complexities of dry sliding wear behaviour of steels. *Mater. Sci. Technol.* **2021**, *37*, 504–518. [CrossRef]
80. Peng, R.; Shen, J.; Tang, X.; Zhao, L.; Gao, J. Performances of a Tailored Vegetable Oil-Based Graphene Nanofluid in the MQL Internal Cooling Milling. *J. Manuf. Process.* **2025**, *134*, 814–831. [CrossRef]
81. Afonso, I.S.; Nobrega, G.; Lima, R.; Gomes, J.R.; Ribeiro, J.E. Conventional and Recent Advances of Vegetable Oils as Metalworking Fluids (MWFs): A Review. *Lubricants* **2023**, *11*, 160. [CrossRef]

Disclaimer/Publisher's Note: The statements, opinions and data contained in all publications are solely those of the individual author(s) and contributor(s) and not of MDPI and/or the editor(s). MDPI and/or the editor(s) disclaim responsibility for any injury to people or property resulting from any ideas, methods, instructions or products referred to in the content.